ADDIS ABABA UNIVERSITY

COLLEGE OF NATURAL AND COMPUTATIONAL SCIENCES

SCHOOL OF EARTH SCIENCES

COMPARATIVE ANALYSIS OF URBAN EXPANSION ON LST AND VEGETATION CONDITIONS OF THE CITY ENVIRONS USING REMOTE SENSING TECHNOLOGY: A CASE OF THREE CITIES IN ETHIOPIA.

A THESIS SUBMITTED TO THE SCHOOL OF GRADUATE STUDIES OF ADDIS ABABA UNIVERSITY IN PARTIAL FULFILMENT OF THE REQUIREMENTS FOR THE DEGREE OF MASTERS OF SCIENCE IN REMOTE SENSING AND GEO-INFORMATICS

BY
PENIEL WACKTOLA
ID: GSR/4375/14

Addis Ababa, Ethiopia

June, 2023

ADDIS ABABA UNIVERSITY

COLLEGE OF NATURAL AND COMPUTATIONAL SCIENCES

SCHOOL OF EARTH SCIENCES

COMPARATIVE ANALYSIS OF URBAN EXPANSION ON LST AND VEGETATION CONDITIONS OF THE CITY ENVIRONS USING REMOTE SENSING TECHNOLOGY: A CASE OF THREE CITIES IN ETHIOPIA.

A Thesis Submitted to the School of Graduate Studies of Addis Ababa University in Partial

Fulfilment of the Requirements for the Degree of Masters of Science

In Remote Sensing and Geo-Informatics

By

PENIEL WACKTOLA

ID: GSR/4375/14

Advisors:

Biniyam Tesfaw (PhD)

K. V. Suryabhagavan (PhD)

Addis Ababa, Ethiopia

June, 2023

Declaration

I hereby declare that the dissertation entitled "Comparative analysis of Urban expansion on LST and vegetation conditions of the city environs using remote sensing technology: A case of three cities in Ethiopia." has been carried out by me under the supervision of Dr. Biniyam.T, School of Earth Sciences, Addis Ababa University, Addis Ababa during the year 2021−2023 as a part of Master of Science programme in Remote sensing and Geo-informatics. I further declare that this work has not been submitted to any other University or Institution for the award of any degree or diploma.

Place: Addis Ababa
Date: June, 2023

(Peniel Wacktola)

ADDIS ABABA UNIVERSITY

School of Graduate Studies

School of Earth Sciences

Comparative analysis of Urban expansion on LST and vegetation conditions of the city environs using remote sensing technology: A case of three cities in Ethiopia.

By PENIEL WACKTOLA

ID: GSR/4375/14

A Thesis Submitted to

The School of Graduate Studies of Addis Ababa University In Partial Fulfilment of the Requirements for the Degree of Masters of Science in Remote Sensing and Geo-Informatics

Approved by Board of Examiner

Prof Worash.G

Chairman	Signature	Date

Dr. Biniyam.T

Advisor	Signature	Date

Dr. K. V. Suryabhagavan

Advisor	Signature	Date

Dr. Tibebu.K

Examiner	Signature	Date

Prof. Bekele.A

Examiner	Signature	Date

ACKNOWLEDGMENTS

First and foremost, I want to express my gratitude and appreciation to my thesis advisors, Dr. Biniyam T. and Dr. K. V. Suryabhagavan, whose insightful comments, kind support, on going mentoring, and feedback made this study possible. I want to express my gratitude to my friends and classmates for their great cooperation and assistance with regards to various materials and concepts. I want to express my gratitude to my husband, family, and friends for their constant encouragement and support during the study.

Comparative analysis of Urban expansion on LST and vegetation conditions of the city environs using remote sensing technology: A case of three cities in Ethiopia.

Peniel Wacktola Teffera, MSc. Thesis

Addis Ababa University, June 2023

Abstract

Population growth has been followed with urbanisation for the past 50 years and this urbanization has impacts on the environment like Land Surface Temperature and vegetation conditions on the urban areas. Therefore, this research aims to evaluate how land use patterns have changed over the past 19 years in three cities and how those changes have affected vegetation and land surface temperature (LST). Satellite images such as Landsat ETM+ (2003 and 2013), Landsat 8 OLI/TIRS (2022) and ASTER night time image were used as geospatial data to extract the Environmental variables (Land Use Land Cover, Normalized Difference Vegetation Index - NDVI, Normalized Difference Built-up Index - NDBI, and LST). Split window algorithm was the method to calculate LST. The result shows that LULC has a decrease change in agricultural areas and increment of built-up areas for the three cities during the study periods. The study indicated that areas having lower LST in 2003 (mean LST = 9.13 ^{o}C , 17.63 ^{o}C, and 12.80 ^{o}C) were changed to higher LST in 2022 (mean LST = 12.19 ^{o}C, 21.97 ^{o}C, and 17.60 ^{o}C)in Addis Ababa, Adama and Hawassa, respectively. Also, the vegetation cover decreases from 25005.78 ha, 7801.48 ha, and 13489.92 ha in 2003 to 13394.23 ha, 3462.16 ha and 6633.87 ha in 2022 in the three cities, respectively. The mean of NDBI in 2003 (Addis Ababa=0.02, Adama=−0.01 and Hawassa =−0.03) and increases to 0.17 in Addis Ababa, 0.11 in Adama and 0.08 in Hawassa for the year 2022. The correlation result (Year 2022) shows that NDBI (Built-up) has a positive correlation (R=0.89, R=0.87 and R=0.91) with LST and a negative correlation (R=-0.62, R=-0.77, and R=-0.86) with NDVI (vegetation) for Addis Ababa, Adama, and Hawassa, respectively. This result gives an insight to Environmental experts and organizations to reduce the impacts of urbanization on the LST and Vegetation in cities and surrounding areas. This study also demonstrated that geospatial tools and methodologies may provide quick and accurate results for analysing environmental variables and change at the regional scale.

Key words: Remote Sensing, Geospatial data, Urbanization, NDVI, NDBI, LST

Table of Contents **Pages**

List of Figures

List of Tables

List of Acronyms

ASTER	Advanced space-borne Thermal Emission and Reflection
CSA	Central Statistical Agency
DEM	Digital Elevation Model
ENVI	Environment for Visualizing Images
ERDAS	Earth Resources Data Analysis System
ETM+	Enhanced Thematic Mapper
FAO	Food and Agricultural organization
GIS	Geographic Information System
Ha	Hectare
Km	Kilometre
LST	Land Surface Temperature
LULC	Land –Use and Land-Cover
LULCC	Land –Use and Land-Cover change
m.a.s.l	Meter above sea level
OLI	Operational Land Imager
RS	Remote sensing
TIR	Thermal Infrared
USGS	United States Geological survey
UTM	Universal Transverse Mercator

List of Appendix

CHAPTER ONE

1. Introduction

1.1 Background of the study

Urbanization is significant type of land use and land cover changes (LULC), which can be defined as local increase in population density accompanied by an increase in per capital energy consumption and significant changes to the local environment. It is thought to be an unavoidable trend in today's world (Pickett, 2001). Urbanization is a frequent phenomenon taking place all over the world, where human being lives. It happens as a result of population growth, economic development and infrastructure improvement in a particular area (Komba & Keribich, 2000). Urbanization is growing in both developed and developing countries. Over the past few decades, growth of cities has been taking place at an alarming pace around the world (VALDIVIEZO-N, 2017). Urban impermeable surface have been significantly growing along with this rapid expansion, which has reduced the amount of pervious surface area, such as green spaces and bare soils (Chithra, 2015).

The world's population is more than three times larger than it was in the mid-twentieth century. The people in 1950 adding 1 billion people since 2010 and 2 billion since 1998. The global population could grow to around 8.5 billion in 2030, and 1.18 billion in the following two decades, reaching 9.7 billion in 2050. More than half of the projected increase in the global population between 2022 and 2050 is expected to be concentrated in just eight countries: the Democratic Republic of the Congo, Egypt, Ethiopia, India, Nigeria, Pakistan, Philippines and the United Republic of Tanzania (UN, 2022). It has been widely observed that humanity is relocating from rural area to cities (Angel, 2011). Rapid urban population growth is leading to massive unplanned spatial expansion on the peripheries of cities. The major loci of urbanization in the coming decades will be Sub-Saharan Africa and South and Central Asia, regions that are expected to add 2.35 billion urban residents by 2050, roughly 13-fold greater than the increase in the remaining world region combined. In Sub-Saharan Africa, this amount to a three-fold increase in the total population living in urban areas in a generation. Urban growth at this scale and speed has occurring in these regions for at least 25 years (Lamson-Hall, 2022).

Rapid urbanization brought on by population increase alters the land use and land cover in many metropolitan regions. In developing nations with rapid population growth rates like Ethiopia, the rate of such transformation is evident. In addition to the altered agricultural areas, these unchecked urban changes around Ethiopian towns have the potential to exacerbate a wide range of social and physical issues. The vegetation cover, hydrological regimes, and local climates all drastically changes as results of urbanization. The increase in land surface temperature (LST) in urban areas compared to the surrounding rural areas is the most visible climatic effect of urbanization (ZHOU & WANG, 2010).

New possibilities for sophisticated environmental management are now being made available through remote sensing (RS) and geographic information system (GIS) or geospatial technologies. Satellite data enable synoptic analysis of the earth system, patterns, and changes from local to global scales across time. Therefore, an effort has been made in this study to assess, examine and map out the state of LULC, vegetation and LST in three cities in Ethiopia. In addition to analysing and processing meteorological data like temperature, remote sensing and geographical information systems are also employed to create crucial information that the relevant body may use as input for environmental management.

1.2 Statement of the problem

Urbanization is major concern in many countries, particularly in Ethiopia where the population is rapidly increasing. The rapid increase of urbanization has led to change in land use, which can have a significant impact on the environment. In particular, urbanization can cause an increase in land surface temperature (LST) and a decrease in vegetation. In particular, urbanization can cause an increase in land surface temperature (LST) and a decrease in vegetation. The increase in land surface temperature can have negative consequences for human health, such as heat-related illnesses and increased energy demands for cooling. It can also affect the environment, leading to changes in weather patterns, reduced air quality, and altered ecosystems. The loss of vegetation can lead to a range of negative consequences, including increased air pollution, decreased air quality, and reduced biodiversity. The loss of vegetation can lead to soil erosion and reduced water quality, as there are fewer plants to absorb and filter rainwater. This can cause flooding and other problems during heavy rainfall events. The study analyze the changes in LST and vegetation these cities, identify the factors that contribute to these changes, and assess the impact of urbanization on the environment. The research use remote sensing data to analyse the changes in LST and vegetation in the three cities and a combination of quantitative and qualitative methods to analyse the factors contributing to the changes. The finding of this study will provide a better understanding of the impacts of urbanization on the environment and provide useful information for policy makers in Ethiopia.

1.3 Objective

1.3.1 General objective

To assess Comparative analysis of Urban expansion on LST and vegetation conditions of the city environs using remote sensing technology: A case of three cities in Ethiopia.

1.3.2 Specific objectives

- ✓ To analyze urbanization, LST and vegetation.
- ✓ To examine land use land cover of Addis Ababa, Adama and Hawasa for specified time periods (2003, 2013, 2022) using object based classification.
- ✓ To analyses the impact of urbanization on surface temperature and vegetation.

1.4 Research questions

- What is the relation between urbanization, LST and vegetation?
- How can land use land cover classify using object based classification for the given time period?
- What is the impact of urbanization on surface temperature and vegetation?

1.5 Significance of the study

This study is significant in two ways: it helps us grasp the potential of remote sensing technologies to assess and monitor the effect of urbanization on the environment. This study will provide insight into the effect of urbanization on the environment by analysing the vegetation and land surface temperature of three cities in Ethiopia: Addis Ababa, Adama and Hawassa. Future urban planning and development attempts can be guided by the researches through assessment of the three cities vegetation and land surface temperature. The information gathered for this study can also be utilized to create urban model that can be used to identify possible environmental problem areas and guide conservation initiatives.

Finally, the result of this study can be used as a reference for other studies examining the impact of urbanization on the environment. This research can provide a baseline for comparison of similar studies in different parts of the world, helping to identify global trends in impact of urbanization on the environment.

1.6 Scope of the study

The purpose of this study was to evaluate the effect of urbanization on LST and vegetation choice RS and GIS technology. The Addis Ababa, Adama and Hawassa cities in Ethiopia were the only ones included in the study's scope.

1.7 Limitations

All appropriate attempts were made to gather the necessary information for the study as primary and secondary data, together with a clear procedural analysis and technical interpretations.

However, this study had the following limitations to deal with:

- Obtaining an appropriate image for the time period specified.
- The standard procedure for obtaining data from various organizations.
- The constrained available internet bandwidth for image downloads.

1.8 Organization of the study

There are five chapters in this study. Introduction (background of the study), statements of the problem, objective the study (general and specific objectives), research questions, significance of the study, scope of the study, limitation of the study and organizational structure of the paper are all included in the first chapter. The second chapter is about literature review. The study area, research methodology, data source, modelling and data analysis are discussed in the third chapter. The result and discussion is covered in the fourth chapter. The final chapter give a conclusion and a recommendation.

CHAPTER TWO

2. Literature review

This chapter summarizes related research that has been done in many geographic areas, as well as the fundamental concept and interconnections between LULCC, LST and NDVI as well as the applications of RS and GIS. Additionally, it makes an effort to examine the results of relevant research that have been conducted in the past in various fields and the gap analysis for the present research topic.

2.1 Remote sensing and GIS

Remote sensing is process of detecting and monitoring the physical characteristics about an object, a place or phenomenon through the analysis of data acquired by a device without contacting the object which is under exploration (Chipman & Lillesand, 2004). The modern use of the term RS has more to do with technical way of collecting airborne and space borne information. The earth observation from airborne platforms has 150 years of history, although the majority of the innovation and development has taken place in the recent decade's years (Zubair, 2006). The first earth observation-using balloons in the 1860s were regarded as an important benchmark in the history of remote sensing (Lillesand, 2008).

At the natural level, information is gathered by tools like cameras or even just our eyes (radiometric which measure radiation). In order to examine the many aspects of the atmospheric environment, climatology, meteorology, ecology, agronomy and environmental protection, satellite-based remote sensing delivers useful information (Kern, 2011). The fundamental function of RS is to measure and record the electromagnetic radiation that the earth's surface emits or reflects (Hardegree, 2006). With the use of this technique, we can look into and determine how LULC tends to change over time.

Geographic information system (GIS) is a computer-based system that is used for data capture and preparation, managing, visualize, analyze and interpret data and it helps to understand trends, patterns and relationships between different types go-referenced data (Huisman & De By, 2009). GIS data types may be divided into two main categories: spatial data and non-spatial data. Data with a location value are considered spatial data, whereas non-spatial data are those that provide a more detailed description of spatial data in the form of a table.

In the 1960s, the combination of cartography and computing technology opened the door to the potential of applying map superimposition and overlay techniques outside of the field of cartography. Manger and scientists alike have access to new and sophisticated models related to the power amplification that comes from the combination of climate, environment, terrain, agronomic, economic, social and institutional management data (Foresman, 1998).

Therefore, it is vital for urban research and development processes to incorporate remote sensing and geographic information system methodologies. If this is done, it will be essential in the construction of effective and affordable models for the growth and allocation of industries, education, housing, water supply, service facilities and disposal system that are relevant to urban studies.

2.2 Urbanization

The physical expansion of urban areas as a result of global change is known as urbanization or urban drift. The United Nations defines urbanization as the migration of people from rural to urban regions, where population growth is equivalent to urban migration. Large city growth, urban concentration, changes in land use and the shift from a rural to a metropolitan style of organization and government are all results of social, economic and political processes.

The 2005 Revision of the UN World Urbanization prospects study details the world's population fast urbanization during the course of the 20th century. Accordingly, the percentage of the world's population living in urban areas increased significantly, from 13% (220 million) in 1900 to 29% (732 million) in 49% (3.2 billion) in 2005. The coming of the "Urban Millennium" or the "tipping point" is when the majority of people on earth will be living in towns or cities for the first time in history, according to the UN State of the world population 2007 report. According to project future trends, emerging countries will experience 93% of global urban expansion, with Asia and Africa accounting for 80% of this growth. The rates of urbanization differ amongst nations. Compared to China, India, Swaziland, Nigeria, the United State and the United Kingdom have a far higher degree of urbanization but a much slower yearly rate of urbanization since a significantly smaller proportion of the population live in rural areas (Table 2.1).

Table 2.1 Urbanization trends by major regions (1950-2050)

Major regions	Urban area percentage				
	1950	1970	2014	2030	2050
Africa	14.4	23.5	40.0	47.7	56.0
Asia	17.5	23.5	47.5	55.5	64.4
Europe	51.3	62.8	73.4	77.4	82.2
Latin America and the Caribbean	41.4	57.1	79.5	83.4	86.0
Northern America	63.9	73.8	81.5	85.8	87.3
Oceania	62.4	71.2	70.8	71.4	74.0

Source: (UN, 2014)

Urbanization in Africa

Urbanisation is accelerating in countries that are both developed and developing. Rapid urbanisation, in especially the growth of large cities, with the associated problems of high unemployment, poverty, poor health, inadequate sanitation, urban slums and environmental degradation constitute a formidable challenge in many emerging countries, though. Despite the fact that urbanization is the primary factor behind modernization, economic progress and growth concerns about the negative consequences of urbanisation notably on the environment, human health and livelihoods are growing. Rapid urbanisation and growth in population have significant impact on employment, food security, housing, water supply, sanitation and particularly how waste(solid and liquid) produced by cities is disposed of. Considering the attendant urban issues of unemployment, slum development, poverty and environmental degradation, particularly in emerging nations the question of weather the current trend in urban in urban growth is sustainable arises (UNCED, 1992).

The majority of Africans move into urban areas either because they are "pulled" there by the benefits and opportunities of city, such as education, electricity, water etc., or because they are "pushed" there by elements like poverty, environmental degradation, religious strife, political persecution, food insecurity, a lack of basic infrastructure and service in rural areas. Young people are typically driven to urban areas by the comforts of city living despite the fact that there are few employment in urban areas in many African nations (Canning, 2015).

Urbanization in Ethiopia

Even by African standards, Ethiopia had a low urbanisation rate. Only approximately 11% of people were residing in metropolitan areas with at least 2000 inhabitants in the late 1980s. Although there were hundreds of towns with 2000 to 5000 residents, they were mainly just rural villages with no urban or governmental powers. So, if one applied stringent urban structural requirements, the level of urbanisation would be considerably lower. The country's history of agricultural self-sufficiency, which has strengthened rural peasant life, is the cause of Ethiopia's relative lack of urbanisation. Up until the Italian invasion in 1935, the pace of urban growth was midst. The Italian occupation of 1936−1941 saw fairly fast urban growth both during and after. The 1960s saw an increase in urbanisation, with an average annual growth rate of approximately 6.3%. The northern half of Ethiopia, where the majority of the major towns are located, was particularly noticeable in terms of urban growth.

The development of relatively new metropolitan centres grew quickly between 1967 and 1975. Six towns- Akaki, Arba Minch, Hawassa, Bahir Dar, Jijiga and Shashemene saw a population increase of more than three times that amount, as did eight other towns. Newly recognised as the administrative region's and significant agricultural hubs, Hawassa, Arba Minch, Metu and Goba. The sidamo region's capital, Hawassa was conveniently situated on the Addis Ababa-Nairobi highway and featured a lakeside setting.

Addis Ababa, DirevDawa and Debre Zeyit are afew examples of more established towns with moderate urban expansion. Some of the older provincial capitals, like Gonder, saw moderate growth as well, but others like Harer, Dese, Debre Markos and Jimma saw their rates of expansion drop due to competition from larger cities. Harer, Dese and Kembolcha were all eclipsed by Dire Dawa by the 1990s and Debre Markos by Bahir Dar.

All urban areas had significant population influx as a result of the escalated fighting between 1988 and 1991, which led to serious overcrowding, housing and water shortages, an overuse of social services and unemployment. In addition to beggars and people with physical disabilities, there were many young people among the new arrivals. A startling number of orphans and street children approximately 100,000 as well as primary and secondary school pupils were also included. All significant towns experienced this inflow, but Addis Ababa-the capital city was hardest hit (Source: U.S Library of Congress).

Ethiopia’s urban population is increasing rapidly. Ethiopia’s urban population share estimated at only 17.3 %in 2012, is among the lowest in the world and far lower than the average for sub-sharan Africa, which 37 %. But this is about to drastically change. The Ethiopian Central Statistic Agency estimates that the urban population will increase by 3.8 % annually from 15.2 million in 2012 to 42.3 million in 2037, or nearly quadruple. According to the analysis for this paper, the rate of urbanisation will be much higher, at roughly 5.4 %annually. By 2034, the urban population would have triple and by 2028, 30% of the population would live in urban regions (Sameh & Guang , 2015).

2.3 Concept and causes of land-use and land-cover change

Due to human-induced factors including urbanization, agriculture and deforestation the earth’s surface has been significant changes in recent decades. Land is the most important resource in the biosphere and several studies have used the terms land-use and land-cover (LULC) to refer to it. These two phrases, however, refer to two distinct problems and have different meanings. The term "land-cover" describes the bio-physical cover that can be seen on the surface of the earth, such as water bodies, plant, soil, and hard surfaces. Land-use is the exploitation or use of the land for human habitation, agriculture, forestry and pastures which changes the land surface processes such as biogeochemistry, hydrology and biodiversity (Di Gregorio & Jansen , 2000). The definition also given by (FAO,1999) for land-use is as the arrangements, activities and inputs people undertake in a certain land-cover type to produce change or to maintain it. Negative socio-ecological feedback resulting from a serious (severe) degradation in ecosystem services as a result of socioeconomic developments and innovations might lead to a transition in LULC (Lambin, & Meyfroidt, 2010). Land-use change first occurs at the level of individual land parcels when land managers decide that a shift toward another land utilization type is desired. Land-cover change is the conversion of the land-cover from one type to another and adjustment of the conditions within a category (Meyer & Turner, 1992).

Land-use change are a reflection of both human history and possibly human destiny. These changes are driven by a number of variables connected to the expansion of human population, economic development, technological advancements and environmental changes (Houghton R. , 1994). One of the main drivers of LULC change is population growth. The most valuable natural resource is people and their sustained growth depends on them in many different ways (Santa , 2011). The amount of land that has been used for agriculture has increased by more than 45% over the past three centuries going from 2.65

million km² to 15 million km², while at the same time other natural resources(land-cover) like forests have been disappearing because of the expansion of agriculture and urbanization (Santa , 2011). High rate of deforestation in many developing countries is most commonly associated with population growth and poverty (Mather & Needle, 2000). Land-use and land-cover changes have become major problems for the world , it is a significant driving agent of global environmental changes (FAO, 1999Such a large-scale land-use classes through the increase of agricultural land at rural area, deforestation (clearance of tree), urbanization and other natural phenomena and human activities are inducing changes in global systems and cycles. However, the major change in land-use, historically has been the worldwide increase in agricultural land (Houghton R. , 1994). Long term or permanent changes to local climate are referred to as climate change. Increased frequency of droughts, a rise in global temperatures, tropical cyclones, floods, decreased yearly rainfall, a loss in the glacier cover of mountains and rising sea level are some of the signs of climate change (Alemayehu , 2008).

United States Environmental Protection Agency (USAPA, 2004), identified the general causes of LULCCs are:

- ✓ Natural processes, such as climate and atmospheric changes, wildfire and pest infestation
- ✓ Direct effect of human activity such as road and illegal house construction and deforestation
- ✓ Indirect effects of human activity is such as, water diversion leading to lowering of the water table

2.4 Land surface temperature (LST)

LST is a measure of how hot land surface at a particular location and it define as the skin temperature of the surface (Latif, 2014). Land surface temperature denotes the temperature on the surface of the earth or it is the skin temperature of the earth surface phenomena (Kayet & Pathak, 2016). From the satellites point of view the surface looks different for different area at different times (Kumar & Singh, 2016). Geospatial and remote sensing tools are essential for assessing and estimating LST. Geometrically corrected land surface temperature can be used to calculate ASTER thermal image from band 10-band14 (Khin & Shin, 2012). Based on a region's brightness temperature and the land surface emissivity, which is estimated using the split window algorithm, it could determine the land surface temperature there (Rajeshwari & Mani, 2014). LST gives information about the difference of the surface equilibrium state and vigorous/vital for many applications (Kerr & Lagouarde, 2004). It is an essential factor in many areas like global climate change studies, urban land-use and land-cover, geo-biophysical and also an input for climate models (Reddy & Manikiam, 2017).

Land surface temperature also defined as, the monitoring of surface temperature based on pixel derived observation through RS (Paramasivam, 2016). Urban land surface temperature is determined by its surface energy balance, which is controlled by factors like orientation, sky and wind, openness to the sun and radioactivity, ability to reflect solar and infrared light as well as the ability to emit infrared light, availability of surface moisture to evaporate and surface roughness (Voogt, 2000).

LST is a key variable to understand the impacts of urbanization induced LULC changes (Fu & Weng, 2016) because it can accurately describe the thermal environment at a city-scale and throughout a specified time period (Li & Song, 2011). Studies have also found that physical processes, such as irradiative fluxes and land surface material characteristics (e.g albedo, emissivity, thermal capacity and conductivity) can clarify the correlations between land cover types and temperature (Yu & Guo, 2015). Rapid urbanization has caused significant land–cover change as well as changes in the land surface temperature because they have a direct correlation in between (Forman, 2016) and different studies show that the process of urbanization has the potential to increase the land surface temperature of a region because impervious surface types have replaced other land use land cover types that have a major cooling effect through the process of evapotranspiration (Tayyebi, 2018; Madanian, 2018; Wang, 2018).

2.5 Normalized difference vegetation index (NDVI)

Normalized difference vegetation Index is based on reflectance measurements in the near infrared (NIR) and Red regions of the spectrum, the vegetation Index is derived as the difference between visible red and near infrared reflectance values normalised across reflectance (Burgan & Hartford, 1993). The NDVI values range from -1 to 1, with the positive value representing reflective surface like vegetation. The negative values represent water, snow, clouds, non-reflective surfaces and other non-vegetated areas (Burgan & Hartford, 1993).

One of the most crucial markers of a regional ecological status is the amount of vegetation. The land surface temperature of a particular area is determined by the vegetation growth circumstances since a high NDVI value denotes a low land surface temperature (LST) due to the latent heat flow from the surface to the atmosphere via evapotranspiration. Generally speaking, locations with high NDVI have lower LSTs (Li, Liu, & Cao, 2015)

As demonstrated by various researches, the relationship between the NDVI value and LST is inverse. Studies show that in order to preserve the urban climate, reduce the impact of urban heat islands(UHI) and support the urban ecosystem, there must be green space or urban vegetation cover (Ibrahim & Rasul, 2017).

2.6 Normalized difference built up index (NDBI)

The Normalized Difference Built-up Index (NDBI) emphasises manufactured built-up areas by using the NIR and SWIR bands. I t is ratio-based to mitigate the impact of variations in terrain illumination and atmospheric effects. Due to its simultaneous use of near infrared (NIR) and short infrared (SWIR), the NDBI is able to show urban built-up areas. Only after the accuracy evaluation procedure may more in-depth examination of NDBI and land-cover changes be done (Muhammad Yazrin Yasin, 2020). Additionally, the value of the NDBI ranges from -1 to 1. Higher NDBI values indicate built-up regions, while negative values indicate water bodies. The vegetation NDBI value is low.

CHAPTER THREE

3. Materials and methods

3.1 Description of the study areas

The research locations are located in Ethiopia Addis Ababa, Adama and Hawassa, two regional capital cities and one metropolitan area (Fig 3.1). The following primary criteria were used to determine which cities were included in this study: (i) being the largest, the capital city or a major metropolitan and regional city; (ii) being relatively the main political, economic and commercial centre of their country; (iii) being a city that is experiencing an increase in industrialization and urbanisation; and (iv) having the highest population in their respective cities.

The city of Adama is located in Ethiopia's oromia region in the centre. The city is located 99km southeast of Addis Ababa, in the East Shewa zone, between the Great Rift valley to east and the base of an escarpment to the west. Adama, Oromia, Ethiopia, has a latitude of 8.514477, a longitude of 39.269257 and a land area of 29.86 km2. Ethiopia's capital, Addis Ababa, is renowned as Africa's diplomatic centre. The area covered by Addis Ababa is 527km2. The city's absolute location are 38°39′03″-38°54′19″E and 8°50′10″-9 ° 06′01″N. On the shores of Lake Hawassa in the Great Rift Valley is the Ethiopian city of Hawassa. It is located 273 km via Bishoftu south of Addis Ababa, 130km east of Sodo and 75 km north Dilla. The town serves as the Sidama Region's capital. It is located on the Trans-African highway 4 Cairo-cape town, with coordinates of 7°3′N and 38°28′E and covers an area of 50km2. Map of the study area is shown in (Fig 3.1).

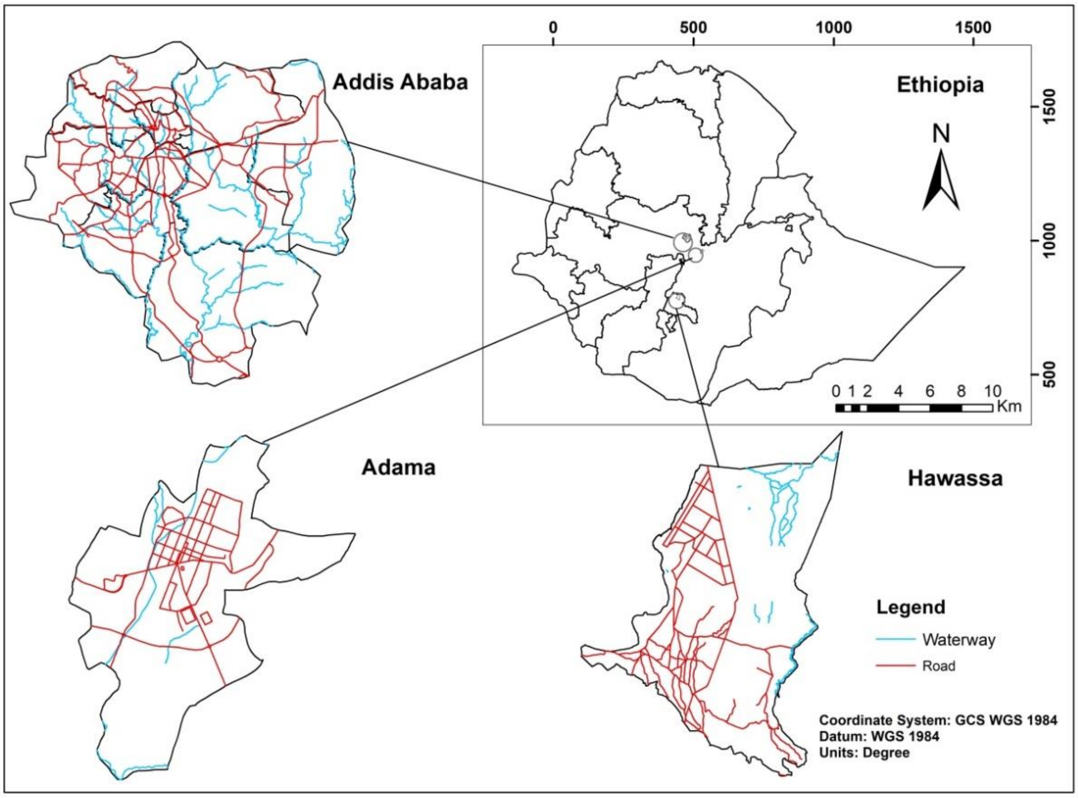

Fig 3.1 Location map of study area (source UN OCHA, 2022)

3.2 Topography

Ground elevations in Adama town range from 1595 m.a.s.l to 1740 m.a.s.l. The lowest area of the town are in its southern central part, where the ground elevation ranges from 1595 m.a.s.l to 1630 m.a.s.l. From the centre of the town to its northern and southern edges, greater altitude regions can be found. These regions range in altitude from 1630 m.a.s.l to 1740 m.a.s.l.

Entoto mountain to the north, Yerer mountain to the east and Wechecha mountaian to the northwest define the boundaries of Addis Ababa. The elevation of the city varies from 2015 m.a.s.l to 3140 m.a.s.l. With elevation of 2015 m.a.s.l and 3140 m.a.s.l respectively Kality and Entoto mountain are home to the lowest and highest points.

Amora Gedele park is situated on the tuff-cone shaped peninsula that forms the southwest corner of Hawassa town. The Chabi peak 2314 m.a.s.l and summit of the Chabi silicic shield volcano is the location's highest point. Lake Hawassa which fluctuates approximately 1685 m.a.s.l is the lowest point.

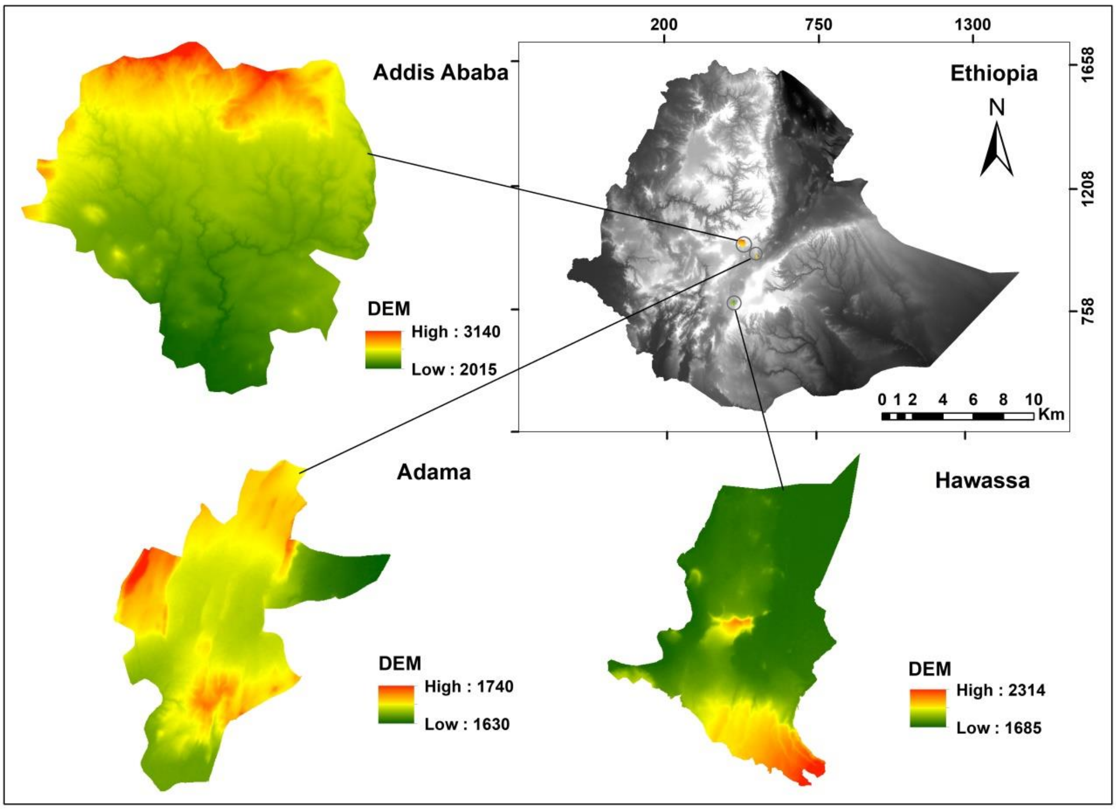

Fig 3.2 Digital elevation model map

3.3 Climate

I. Rain fall

The tropical Great Rift Valley is where Adama town is located. Gena/ kremt(raniy period), Bona/ Bega(dry period), Belg(Little rains) and Meher(a period in between the long and tiny rains) are the four climate seasons. It rains the most in July and August. Rainfall averages are 230mm in July and 235mm in August.

The short rainy season in Addis Ababa lasts from February to April. The city main winter season is the lengthy wet season, which lasts from June to mid-September. Despite the fact that it is summer during this time the temperature are significantly lower than they are during other times of the year due to frequent rain and hail, the Extensive cloud cover and fewer hours of sunshine.

Hawassa experiences warm temperature year-round with variation in the seasons. It has a brief dry season from November to February and a long wet season that lasts from March to October. With an average yearly rainfall of 185mm the months April and May are the wettest.

II. Temperature

In Adama the daily temperature varies between 5.5 °C during November, December and 35°C during March to May. The mean annual ambient temperature is between 19°C to 22°C. Maximum temperature usually occur in March to May. The mean monthly maximum exceeds 30°C. Minimum temperatures are at their lowest in November.

The climate of Addis Ababa is sub-tropical highland, with monthly variations in temperature. Depending on height and dominant wind patterns the city features a diverse mix of alpine climate zones with temperature variations of up to 10°C. Because of the city's proximity to the equator and high elevation, temperature are consistently moderated throughout the year. As a result, the climate would be marine if the height were to be ignored, as no month's mean temperature rises above 22°C. Mid-November to January is when it tends to rain on and off. This id Addis Ababa's dry season, which is typical of highland climate locations with dry winters. The daily highs during this time of year often don't exceed 23°C. The coldest temperature ever recorded was 0 °C, Which was reported on numerous occasions, while the highest temperature ever recorded was 30.6 °C on February 26,2019. In Hawassa the mean maximum and minimum annual temperature are 38.47°C and 7.06°C respectively.

3.4 Population

According to the CSA 2007 census, there are 220,212 people living in Adama, an increase of 72.25% over the number of people counted in the 1994 census. Of these people 108,872 are males and 111,340 are women. Adama has a size of 29.86 km2 with a population density of 7,374.82 people, all are urban inhabitants. In this city there are 60,174 households or an average of 3.66 people per family and 59,431 housing units.

A total of 2,739,551 people live in Addis Ababa's urban and rural areas, according to the national statistics office of Ethiopia 2007 population census. There were 662,728 households in the capital city's 628,984 dwelling units, representing an average of 5.3 people per household.

133,123 and 125,685 women made up Hawassa's total population of 258,808 according to the national statistics office of Ethiopia 2007 population census. The majority of the people in this town 157,879 or 61%, resided in the city of Hawassa but the rest of the population were spread out throughout the rural kebeles nearby. There was an average of

4.22 people per home 57,469 dwelling units among the 61,279 households that were counted in this town.

3.5 Materials

3.5.1 Data Sources and types

In this study, Landsat satellite imagery from the Enhanced Thematic Mapper plus (ETM+) satellite in 2003 and 2013, as well as the operational Land Imager/Thermal Infrared (OLI/TIRS) satellite from 2022, were used. In this study, the same level of resolution Landsat imageries with the ETM+ and OLI-TIRS were collected between January and March 2003, 2013 and 2022. These Land sat images have a 30 meter resolution. I used the image to determine NDVI, NDBI and land use land cover. Additionally, I used Advanced space borne Thermal Emission and Reflection (ASTER) satellite day and night images from the years 2003, 2013 and 2022 to estimate the land surface temperature. These ASTER images have a resolution of 15 meters in the visible and near infrared spectrum and 90 meters in the thermal infrared spectrum. The satellite images were projected using the WGS 1984, zone 37N datum and the Universal Transverse Mercator (UTM) projection. Also , for mapping the elevation, Digital Elevation Model (DEM) data with a resolution of 30*30m was used. Finally, metrological data from Ethiopia’s National Meteorological Service Agency were also used to determine the study area’s minimum, maximum temperature and precipitation values. The Landsat and Aster data source and acquisition data is summarized in (Table 3.1 and Table 3.2).

Table 3.1 Land sat data type and acquisition date

	Satellite image	**Sensor**	**Date of acquisition**	**path and row**	**Cloud cover**
Addis Ababa & Adama	Land sat 7	ETM+	2003/01/12	168/054	0
	Landsat 7	ETM+	2013/02/08	168/054	0
	Landsat 8	OLI	2022/03/13	168/054	0.29
Hawassa	Landsat 7	ETM +	2003/01/12	168/055	0
	Landsat 7	ETM +	2013/02/08	168/055	1
	Landsat 8	OLI	2022/03/29	168/055	0.25

Table 3.2 ASTER data type and acquisition date

	Date of acquisition	Day or Night	Path and row	Cloud cover
Adama	2003/02/03	Night	41/190	1
	2013/01/29	Night	41/190	1
	2022/07/01	Night	41/190	6
	2003/01/12	Day	168/54	0
	2013/10/22	Day	168/54	1
	2022/04/06	Day	168/54	1
Addis Ababa	2003/01/09	Night	41/190	7
	2003/10/08	Night	41/190	8
	2021/12/05	Night	42/190	1
	2002/11/16	Day	168/54	5
	2021/11/20	Day	169/54	3
	2002/12/08	Night	42/189	4
Hawassa	2012/01/18	Night	42/189	1
	2022/03/02	Night	42/189	1
	2002/11/16	Day	168/55	4
	2002/11/16	Day	168/55	1
	2013/12/09	Day	168/55	0
	2021/11/20	Day	168/55	7
	2021/11/20	Day	168/55	1

3.5.2 Tools

The following hardware and software were also used in order to accomplish the objectives of this study.

A. Hardware

- Laptop with an Intel(R) Core(TM) i7-8565U CPU running at 1.8 GHz or 1.99 GHz, 8.00 GB of installed RAM and a 64-bit operating system.
- External Hard disc: 1TB storage size.

B. Software

- Are GIS 10.8: used for preparing maps and analyzing spatial data.
- ERDAS IMAGINE 2015: for remote sensing application to process multi-temporal satellite image including image correction, enhancement, processing (NDBI and NDVI calculation),
- Microsoft Office packages : the thesis was written using which was also used to create data spreadsheets, manage databases, create presentations and print the ruslt.
- Google Earth pro: used for collection of ground truth point for accuracy assessment.
- Quantum GIS (QGIS3.22.1): used for obtaining ASTER satellite image.

- ENVI 5.3: used for LST calculation.
- Saga 7.8.2: used for Object based image classification.

3.6 Methodology

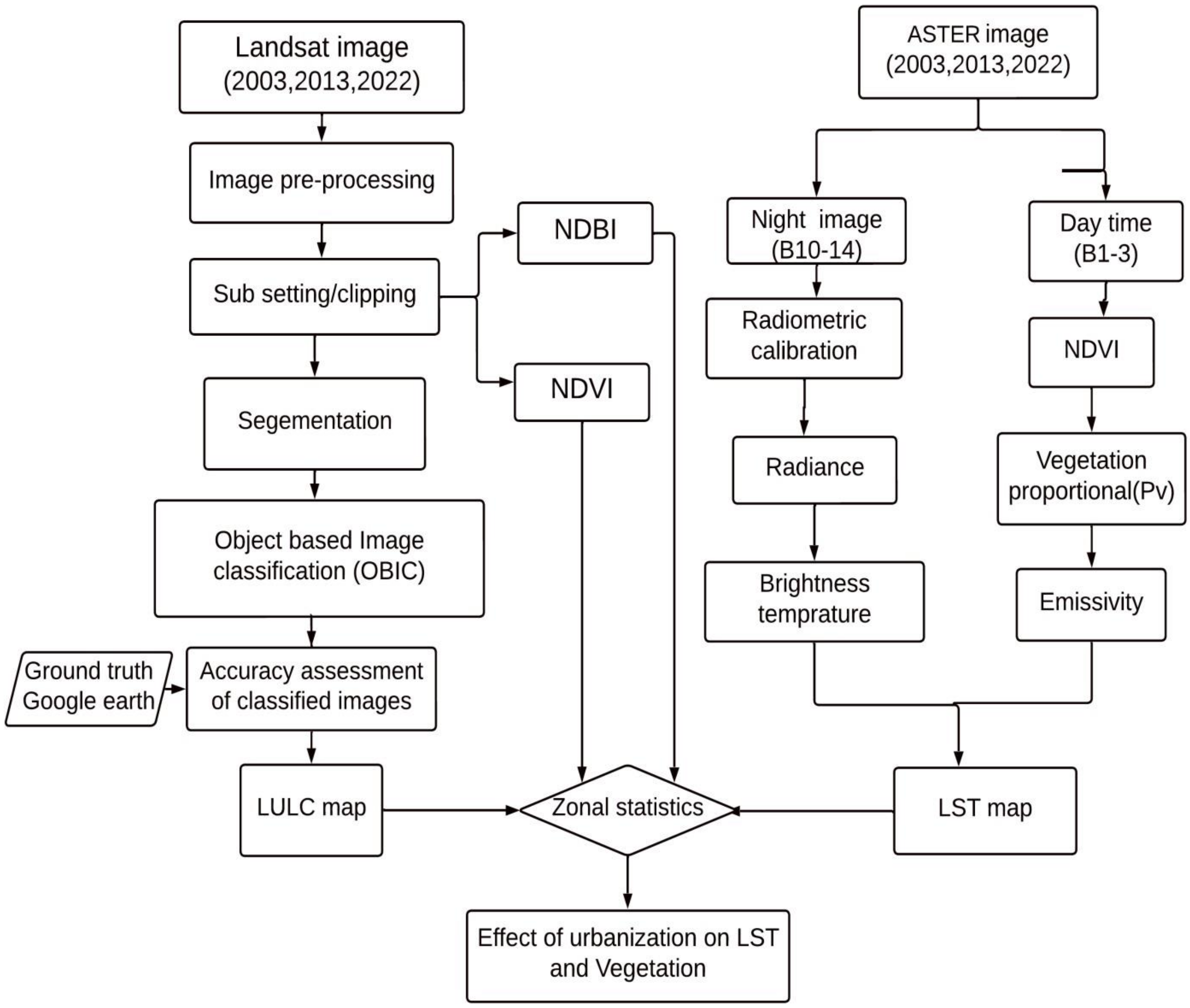

Fig 3.3 Methodological flow chart

3.6.1 Image pre-processing

By improving the apparent distinction between the features, image enhancement aims to enhance the overall visual interpretability of an image. By reducing noise and blur, enhancing contrast and bringing out details, images enhancement makes images easier for human view. Visually interpreting imagery that has been digitally improved makes an effort to maximize the complementing abilities of the human mind and the computer. The mind is great at interpreting spatial attributes on an image and is capable of identifying out difficult-to-see details (Lillesand & Kiefer, 2017).). By nature itself, satellite images contain some distortion, noise, haze and stripes. Consequently, image pre-processing operations were carried out before processing the data. The pre-processing process includes importing, layer staking, sub-setting the image according to the study areas, geometric correction, radiometric correction, scan line error correction, pan sharpening and other image enhancing methods. To make the ground truth conditions based on the sensory move representative, atmosphere noise is removed by radiometric correction. By improving apparent difference between the scene's aspects, the activities mentioned above were aimed to make an image easier to visually interpret. All included geometric correction, radiometric correction, scan line error correction, pan sharpening and other image enhancing methods activities were applied using the software ERDAS IMAGINE 2015.

After all corrections are done the researcher clipped the Area of interest (AIO)/study area. In remote Sensing, it means the area showed in the remote Sensing image. When the Landsat and ASTER image is downloaded from USGS online service the image were cover large area beyond the study area so the AIO/ study area should be sub-sated/clipped by using the shape file or boundary of the study area by using ERDAS IMAGINE 2015 software's.

3.6.2 Image classification

The image classification is a procedure, where we categorize the pixels of the satellite data into various land cover classes, known as the information classes. The objective of image classification is to classify features in an image according to the type of ground cover that is present. The fundamental premise behind obtaining this data is that each item or surface, such as a body of water, an agricultural field, or a fallow piece of land, has distinctive reflectance, absorbance, emittance, and radiation in the visible, near-infrared, and thermal regions of the electromagnetic spectrum. Thus, the image classification or extraction of information is based on spectral, radiometric and spatial differentiation. In other words, image classification is the process of grouping spectral classes and assigning them informational class names.

Spectral and geographical data are both used in object-based or object-oriented classification. The method entails classifying pixels according to their spectral properties, shape, texture and spatial relationship with surrounding pixels. When compared to traditional, pixel-based classification techniques, object-based methods were created relatively recently. While pixel-based classification relies only on the spectral data contained in each individual pixel, object based classification uses data from group of related pixels known as objects or image objects. Groups of pixels that are comparable to one another in terms of their spectral characteristics, such as colour, size, shape, and texture, as well as the context of the pixels' surrounds, are called image objects or features. The process of object-based classification involves segmenting or dividing an image into distinct objects or features, followed by the classification of each object. An essential step in object-based classification is image segmentation. Segmentation is a technique that separates the pixels in an image into groups, objects, or features with related spectral and spatial characteristics. Multiple pixels are present in each of these elements. Ideally, the image's parts match characteristics seen in the real world. An image is classed by assigning each item to a class based on attributes and criteria supplied by the user after the picture has been segmented into suitable image objects.

Techniques for classifying images come in several forms. But in the majority of cases, the researchers divided them in to two main categories: supervised classification and unsupervised classification. Unsupervised classification is the technique employed in this study, which determine if each image in a dataset belongs to one of the innate categories present in the image collection without the assistance of labelled training samples. For the land cover classes this study performs classification using Iso-data clustering algorithm which is a commonly used method in remote sensing for land-use and land-cover classification. This method is based on the clustering of pixels in an image based on their spectral characteristics. It works by first selecting a set of initial cluster centres randomly throughout the image. The algorithm then iteratively updates the cluster centres based on the mean values of the pixels within each cluster. The pixels are then reassigned to the closest cluster centre based on their spectral similarity. This process continues until the cluster centres no longer change or predetermined number of iterations is reached. Advantages of Iso-Data clustering include unsupervised image classification. First off, it is a good method for exploratory analysis because it doesn’t need any training data or prior knowledge. Second, Compared to other approaches, it is relatively quick and can handle huge data sets with ease.

3.6.3 Accuracy assessment

A closeness of result of observations, computation or estimates to the true value or the value accepted as being true is called accuracy assessment. Its mandatory for classification results is because LULC maps contain some errors due to several factors that range from initial data acquisition procedure to the implementation of classification technique (Foody, 2022). The inaccuracies must be quantitatively explained in terms of classification accuracy in order to make sensible use of the remote sensing-derived land cover maps and the supporting land resource statistics. Omission or commission errors are the most frequent types of error in image categorization. An error matrix, often known as a confusion matrix is the most popular way to illustrate classification accuracy. Using error matrix to represent accuracy is recommended and adopted as the standard reporting convention (Congalton, 1991). It presents the relationship between the classes in the classified and reference maps. The technique provides some statistical and analytical approaches to explain the accuracy of the classification. Kappa coefficient, which is one of the most popular measures in addressing the difference between the actual agreement and change agreement, is also calculated. The kappa is a discrete multivariate technique used in accuracy assessment. A number of descriptive and analytical statistical techniques can then be used to the error matrix as a starting point. (Congalton, 1991).

By contrasting the map produced by RS analysis with a reference map based on various information sources, the accuracy of the map is evaluated. A basis for evaluating the LULC classification accuracy was Google Earth. The researcher conducted ground truth point using Google Earth in the study area, identifying randomly 130 points for Addis Ababa and 100 points each for Adama and Hawassa. For the years 2003, 2013 and 2022 LULC map's final output of classification accuracy was calculated.

3.6.4 Land-use and land-cover description

Several factors affect the kind and quality of land use classes. The key determining factor is the impact of the land use category on the recorded changes. This is strongly related to the shared land use area in the town, where other land use categories are immediately distinguishable and recognizable as they change. Once more, local geographical characteristics are grouped together. Land use/land cover nomenclatures are necessary to first construct and define the potential land use /land cover classifications used in this paper are taken from widely used AFRICOVER land use/land cover categorization scheme in East African nations (AFRICOVER, 2002). Given the range of land use land covers in the study area, the researcher simplified the descriptions of some of the land use/land cover classification. The final land use/land cover map of the research region is therefore created using five key nomenclatures: built-up/urban areas, agricultural lands, forests, open space and water body.

Table 3.3 LULC classes and description of the study area

Land cover	**Descriptions**
Water body	All water bodies, marshes, swamps, artificial lakes and ponds.
Forest	Areas covered by dense forest with relatively darker green colures, deciduous forest, mixed forest lands, scrub and others
Agricultural lands	Crop land, pasture and other agricultural land
Built up	Residential, commercial and services, industrial, transportation, roads, mixed urban, and other urban
Bare land	Barren and rocky areas

3.6.5 Land-use and land-cover change detection

Image from 2003, 2013 and 2022 were used to detect changes to the land use, land cover and land cover type. Thematic image comparisons were made using GIS techniques. One of the most used methods for change detection is post classification (Chen, 2000). ArcGIS software were used for technical integration procedures in the evaluation of LULC maps. Creating a table with the area coverage in hectares and the percentage change between 2003, 2013 and 2022 as compared to each LULC class was the first task. As a result (eq.1) a percentage equation was utilized to calculate LULCC (Lambin & Turner, 2001).

$$\text{Percentage change} = \frac{\text{observed change} \times 100}{\text{sum of Area}} \tag{1}$$

3.6.6 Normalized Difference Vegetation Index (NDVI)

The reason NDVI relates to vegetation is that, the one which is well vegetated reflects better in the near infrared part of the spectrum. The value of NDVI is between -1 to 1. NDVI was acquired from spectral reflectance measurements in the visible (Red) and near infrared region (NIR).

$$\text{NDVI} = \frac{\text{NIR} - \text{R}}{\text{NIR} + \text{R}} \tag{2}$$

where: NDVI is normalized difference vegetation index, NIR is near infrared, R is red

Data for Landsat 7, NDVI = (Band 4-Band 3)/(Band 4+Band 3)

Data for Landsat 8, NDVI = (Band 5-Band 4)/(Band 5+Band 4)

For the Landsat sensors ETM+ 2003 and 2013, band 3 is for red and band 4 is for near infrared; however, for the OLI 2022 sensor, band 4 is for red and band 5 is for near infrared.

3.6.7 Normalized Difference Built-Up Index (NDBI)

The normalized difference built-up index (NDBI) emphasizes artificial built-up regions by using the NIR and SWER bands. It is ration based to mitigate the impact of variations in landscape illumination and atmospheric effects. Lower values correspond to aquatic bodies, whereas larger values correspond to built-up regions. NDBI values range from -1 to 1. The vegetation NDBI value is low.

$$\mathrm{NDBI}=\frac{(\mathrm{SWIR} - \mathrm{NIR})}{(\mathrm{SWIR} + \mathrm{NIR})} \quad (3)$$

where: NDBI id normalized difference built-up index, SWIR is short wave infrared, NIR is near infrared

Data for Landsat 7, NDBI= (Band 5-Band 4)/ (Band 5+Band 4)

Data for Landsat 8, NDBI= (Band 6-Band 5)/ (Band 6+Band 5)

For the Landsat sensors ETM+ 2003 and 2013, band 4 is for near infrared and band 5 is for short wave infrared; however; for the OLI 2022 sensor, band 5 is for near infrared and band 6 is for short wave infrared.

3.6.8 Land surface temperature (LST)

To monitor surface energy and water exchange processes at the land atmosphere interface, information regarding land surface temperature (LST) obtained from remote sensing satellite data is crucial (Zhao, 2019). In addition, it is a key variable to be retrieved from the Thermal Infrared data because is widely used in many scientific fields including evapotranspiration, climate change, hydrological cycle, vegetation monitoring, urban climate and environmental among others.(Jiménez-Muñoz, 2008) (Cristóbal, 2009). The LST variable measures the energy exchange between the earth’s surface and atmosphere as well as the amount of radiation emitted from the earth’s surface and sub-surface (Weng, 2019). The TIR region offers a chance to obtain more about this variable using remote sensing. In this regard, numerous efforts have gone into developing techniques for extracting the LST from remote sensing data. According to (Li Z. , 2013) and (Du, 2015), these algorithms can be divided into three categories: (i) single-channel (SC), (ii) multichannel, and (iii) multi-time methods. Group (ii) contains the split-window (SW) methods. The SW methods use fie TIR bands typically located in the atmospheric window. The average wavelength of ASTER satellite image for thermal bands is approximately 8-12 micrometers.

In this study, the land surface temperature was drived by using split-window(SW) algorithm from ASTER night time thermal infrared sensor data. Night time images are more accurate for land surface temperature because during the day, solar radiation heats up the surface and the atmosphere, causing temperature fluctuations and making it difficult to accurately measure land surface temperature. At night, there is no solar radiation and land surface temperature is more stable, allowing for more accurate measurements. Additionally, the split window algorithm used for ASTER night images takes into account atmospheric effects that can impact temperature readings during the day, further increasing the accuracy of the measurements. After these images were collected, NDVI was derived by using band 2 and band 3 ASTER day time image for the year 2003, 2013 and 2022. Digital numbers (DN) were converted to spectral radiance. Finally, land surface emissivity and satellite brightness temperature were estimated and used to calculate land surface temperature.

$$\mathrm{NDVI} = \frac{\mathrm{NIR-R}}{\mathrm{NIR+R}} \tag{4}$$

where: NIR and R (near-infrared band and red band) are band 2 and band 3 of ASTER image 2003, 2013 and 2022.

Aster night time products were also used to estimate land surface temperature. For this ASTER night time images of 2003, 2013 and 2022 respectively were converted to spectral radiance by using;

$$L\lambda = \mathrm{MLQcal} + \mathrm{AL} \tag{5}$$

Where: $L\lambda$ is TOA spectral radiance (watts/(m^2*rad*μm)), ML is band specific multiplicative rescaling factor, AL is band specific additive rescaling factor, Qcal is Quantized and calibrated standard product pixel values(DN).

Spectral radiance was further used to compute at satellite brightness temperature. ASTER bands of 2003, 2013 and 2022, respectively were converted from spectral radiance to brightness temperature by using the thermal bands 10,11, 12, 13 and 14.

$$T = \frac{K2}{\ln(\frac{K1}{L\lambda}+1)} \quad (6)$$

where: T is satellite brightness temperature(0K), Lλ is TOA spectral radiance (watts/(m^2*rad*µm)), K1 is band specific thermal conversion constant, K2 is band specific thermal conversion constant.

By using the cell statistics tool in ENVI, the mean at satellite temperature for bands 10, 11, 12, 13 and 14 was calculated. Land surface emissivity (ε) was computed using the following formula;

$$\varepsilon = 0.004Pv + 0.986 \quad (7)$$

where: (Pv) is the proportion of vegetation and can be calculated as:

$$Pv = [\frac{NDVI-NDVImin}{NDVImax-NDVImin}]^2 \quad (8)$$

where: NDVImin and NDVImax are minimum and maximum NDVI, respectively.

Finally, the emissivity corrected land surface temperature was estimated by using the following mathematical formula;

$$LST = \frac{Tsensor}{1+(\lambda \times T\ sensor\ /\rho)ln\varepsilon} \quad (9)$$

Where: λ is wavelength of emitted radiance (11.3), Tb is brightness temperature(kelvin), ρ is 1.438 $\times 10^{2}$mk and ε is emissivity.

3.6.9 Zonal statistics

The values of raster cells occurring inside zones marks by another raster or vector dataset are used to construct zonal statistics. Zonal statistics condense the data of a specific cell group (Rose, 2022). Zones are all of the input regions with the same values. The zonal statistics function summarizes the value of raster inside the zones of another dataset(either raster or vector) and presents the results as a table and a graphic. Maps for the LULC and LST were made for the years 2003, 2013 and 2022. The zonal statistics tool of the Arc GIS 10.8 was used to evaluate the spatial variation of LST according to different LULC.

Excel was then used to analyses the condensed LULC and LST map data. One of the key approaches used to evaluate the relationship between LULC and LST is the use of zonal Statistics as a table and figure.

CHAPTER FOUR

4. Results

4.1 Land-use and land-cover change in 2003, 2013 and 2022

4.1.1 Addis Ababa land-use and land-cover

According to the 2003 results of the land-use/land-cover classification, agricultural land, bare land, and built-up areas were the three main LULC classes. Agricultural land made up 22800.26 ha (42.2%) of the total area of 53940.11 ha, bare land made up 13562.614 ha (25.1%), and built-up land made up 11693.43 ha (21.6%). collectively, the forest and water body made up the other LULC classifications, which collectively made up 5852.45 ha (10.7%) of the total area.

The results of the 2013 land-use/land-cover classification indicated that agricultural land, bare land, and built-up areas were the three most common LULC classes. Agricultural land made up 15286.34 ha (28.3%) of the total area of 53940.11 ha, bare land 11028.19 ha (20.4%), and built-up land 22307.94 ha (41.3%). The combined area of the other LULC classes forest and water body was 5373.99 ha (9.9%) of the total area.

The results of the 2022 classification of land use and land cover likewise indicated that built up and agricultural land were the major LULC classes. 10037.04 hectares (18.6%) of the total area of 53940.11 ha was made up of agricultural land, and 34766.1 ha (64.6%)was made up of built-up areas. collectively, the forest, bare land, and water body made up the other LULC classes, which collectively made up 9013.46 ha (16.6%) of the total area. Table 4.1, Figure 4.1 and Figure 4.2 shows detailed statistical data for each of these classes and a LULC map of the study period.

Table 4.1 land-use and land-cover classes and area coverage of Addis Ababa

LULC classes	2003		2013		2022	
	(Area)Ha	(Area)%	(Area)Ha	(Area)%	(Area)Ha	(Area)%
Water body	3646.93	6.7	1952.39	3.6	3337.29	6.1
Forest	2205.52	4	3420.6	6.3	3357.19	6.2
Built up	11693.43	21.6	22307.94	41.3	34766.1	64.6
Bare land	13562.14	25.1	11028.19	20.4	2318.98	4.3
Agricultural land	22800.26	42.2	15286.34	28.3	10037.04	18.6
Total	53940.11	100	53940.11	100	53940.11	100

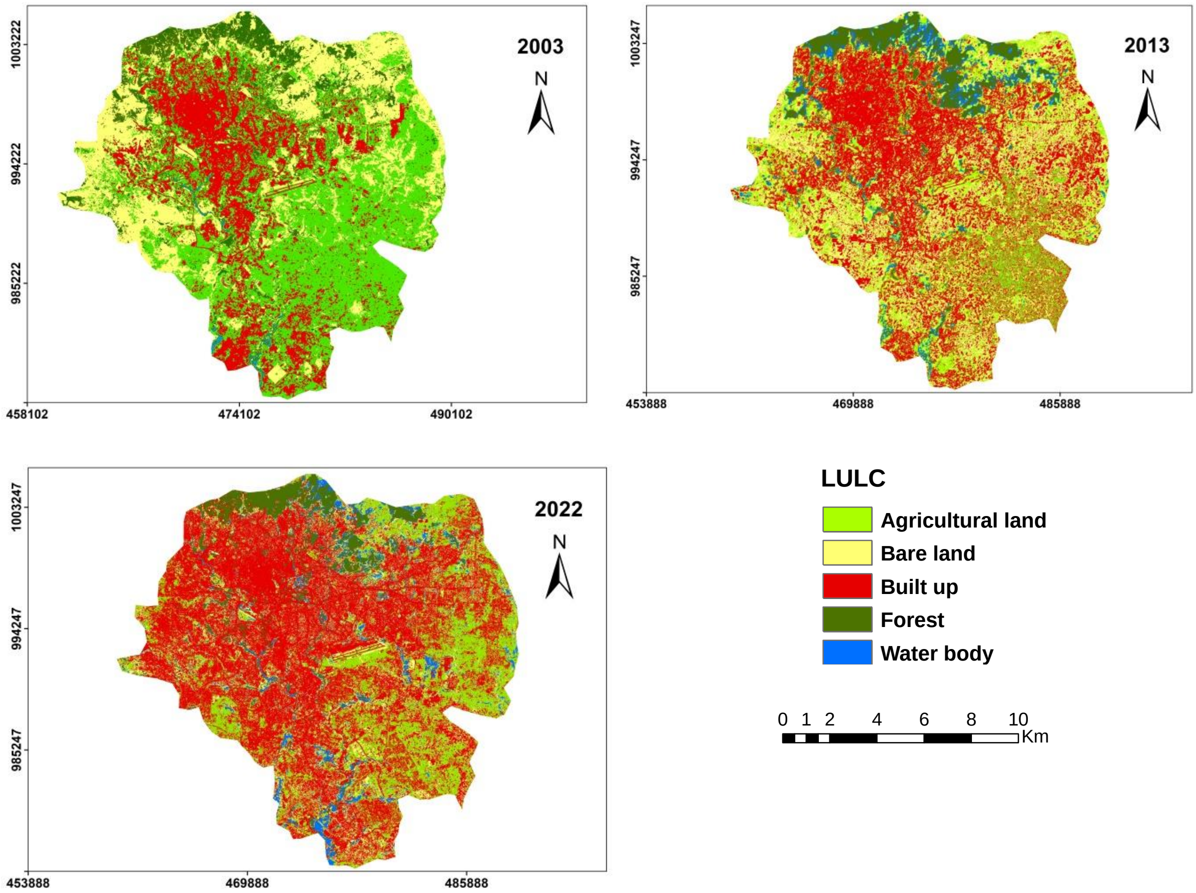

Fig 4.1 Land-use and land-cover of Addis Ababa city

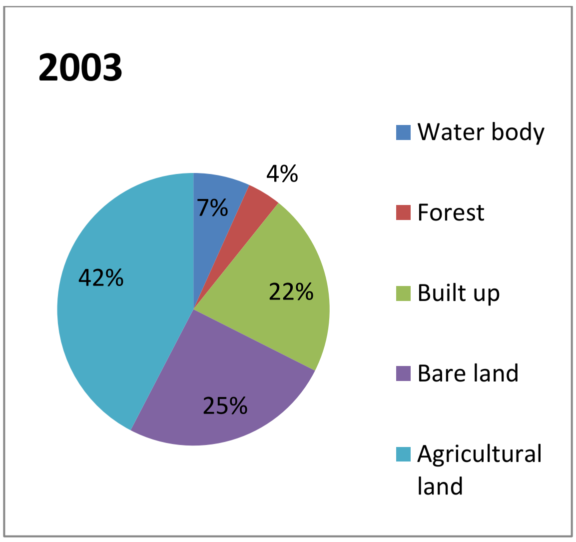

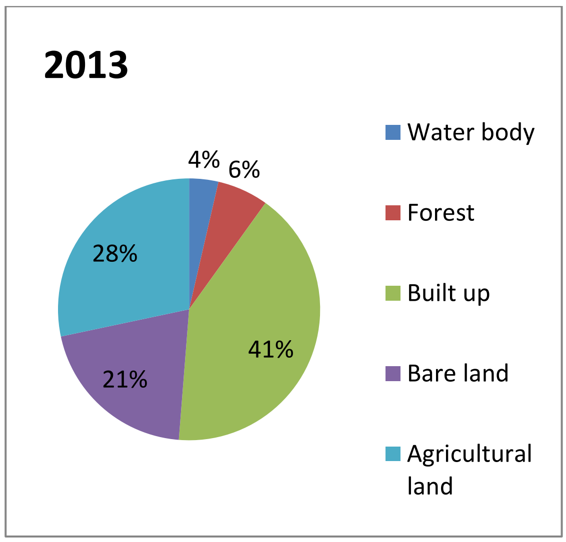

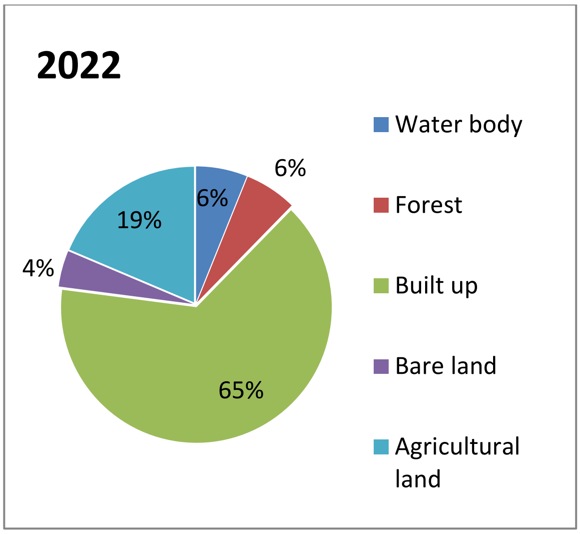

Fig 4.2 Pie-chart of land-use and land-cover of Addis Ababa city

4.1.2 Adama land-use and land-cover

The three main LULC classes identified by the Adama classification's 2003 findings were built-up regions, bare land, and agricultural land. Of the total area of 10976.2 ha, agricultural land accounted for 7090.24 ha (64.5%), bare land for 1230.05 ha (11.1%), and built-up land for 1660.7 ha (15.1%). The remaining LULC classes included the woodland and water body, which together accounted up 1005.22 ha (9%) of the total area.

The three main LULC classes, according to the 2013 results of the Adama classification, were built-up areas, bare land, and agricultural land. Of the total area of 10976.2 ha, agricultural land accounted for 5608.41 ha (51%) while bare land made up 2492.05 ha (22.6%) and built-up land 1972.48 ha (17.9%). The remaining LULC classifications included the forest and water body, which together accounted for 921.14 ha (8.3%) of the total area.

The three main LULC classes, according to the 2012 results of the Adama classification, were built-up areas, bare land, and agricultural land. Of the total area of 10976.2 ha, agricultural land made up 2389.07ha (21.8%), bare land made up 2777.54ha (25.3%), and built-up land made up 4281.18ha (39.1%). The remaining LULC classifications, which included the forest and water body together, accounted up 1500.23 ha (13.7%) of the total area. Table 4.2, Figure 4.3 and Figure 4.4 show detailed statistical data for each of these classes and a LULC map of the study period.

Table 4.2 Land-use and land-cover classes and area coverage of Adama

LULC classes	2003		2013		2022	
	(Area)Ha	(Area)%	(Area)Ha	(Area)%	(Area)Ha	(Area)%
Water body	293.98	2.6	176.89	1.6	427.14	3.9
Forest	711.24	6.4	744.25	6.7	1073.09	9.8
Built up	1660.7	15.1	1972.48	17.9	4281.18	39.1
Bare land	1230.05	11.1	2492.05	22.6	2777.54	25.3
Agricultural land	7090.24	64.5	5608.41	51	2389.07	21.8
Total	10976.2	100	10976.2	100	10976.2	100

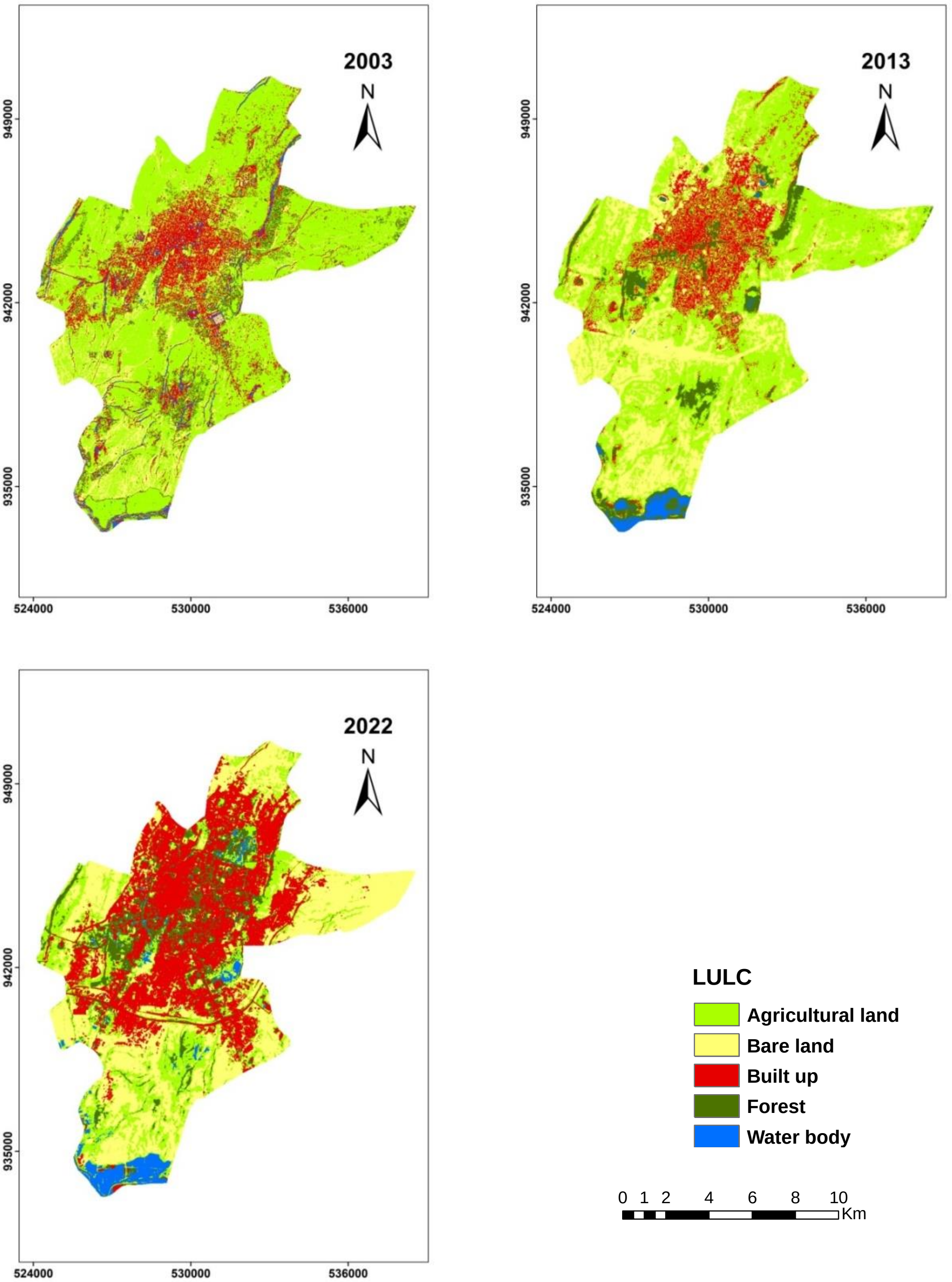

Fig 4.3 Land-use and land-cover of Adama

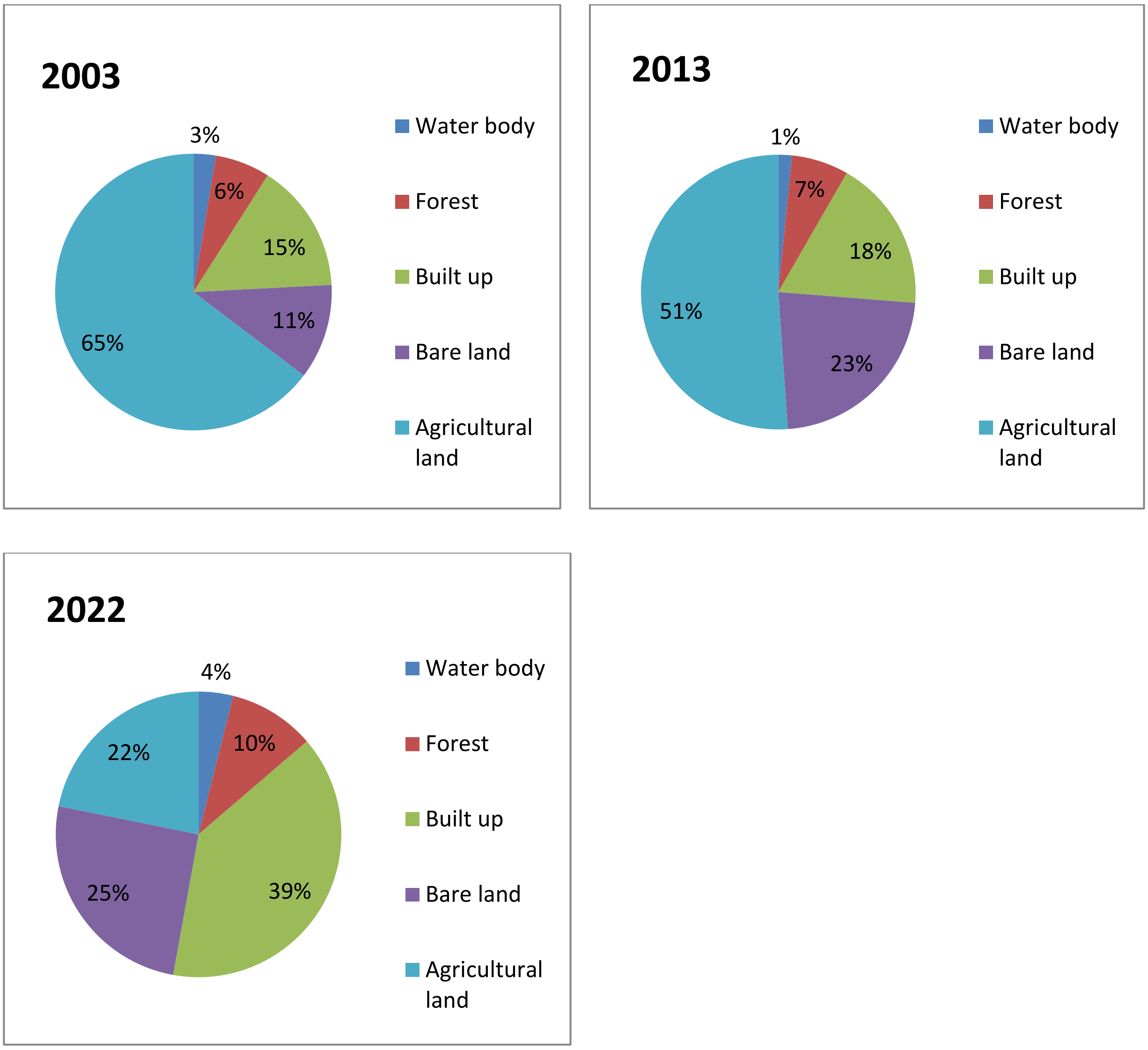

Fig 4.4 Pie-chart of land-use and land-cover of Adama city

4.1.3 Hawassa land-use and land-cover

The results of the 2003 land-use/land-cover classification of Hawassa indicated that agricultural land and forest were the two dominant LULC classes. Agricultural land made up 4836.51 ha (28.9%) of the total area of 16704.95 ha, and forest 8653.41 ha (51.8%). The combined area of the other LULC classes bare land, built up and water body was 3208.94 ha (19%) of the total area.

The results of the 2013 land-use/land-cover classification of Hawassa indicated that agricultural land and forest were the two dominant LULC classes. Agricultural land made up 9104.37 ha (54.3%) of the total area of 16704.95 ha, and forest 3377.95 ha (20.1%). The combined area of the other LULC classes bare land, built up and water body was 4254.59 ha (25.3%) of the total area.

According to the Hawassa classification results for 2022, built-up areas, bare land, and agricultural land were the three dominant LULC classifications. Agricultural land made up 4094.7 ha (24.5%) of the total area of 16704.95 ha, while bare land made up 414.71 ha (24.6%) and built-up land made up 5471.03 ha (32.8%). The forest and water body were the only remaining LULC classes, and they together made up 2998.66 ha (17.2%) of the total area. Table 4.3, Figure 4.5 and Figure 4.6 show detailed statistical data for each of these classes and a LULC map of the study period.

Table 4.3 Land-use and land-cover classes and area coverage of Hawassa

LULC classes	2003		2013		2022	
	(Area)Ha	(Area)%	(Area)Ha	(Area)%	(Area)Ha	(Area)%
Water body	412.83	2.4	1008.24	6	459.49	2.7
Forest	8653.41	51.8	3377.95	20.1	2539.17	15.2
Built up	1164.17	6.9	1433.15	8.5	5471.03	32.8
Bare land	1631.94	9.7	1813.2	10.8	4114.71	24.6
Agricultural land	4836.51	28.9	9104.37	54.3	4094.7	24.5
Total	16704.95	100	16704.95	100	16704.95	100

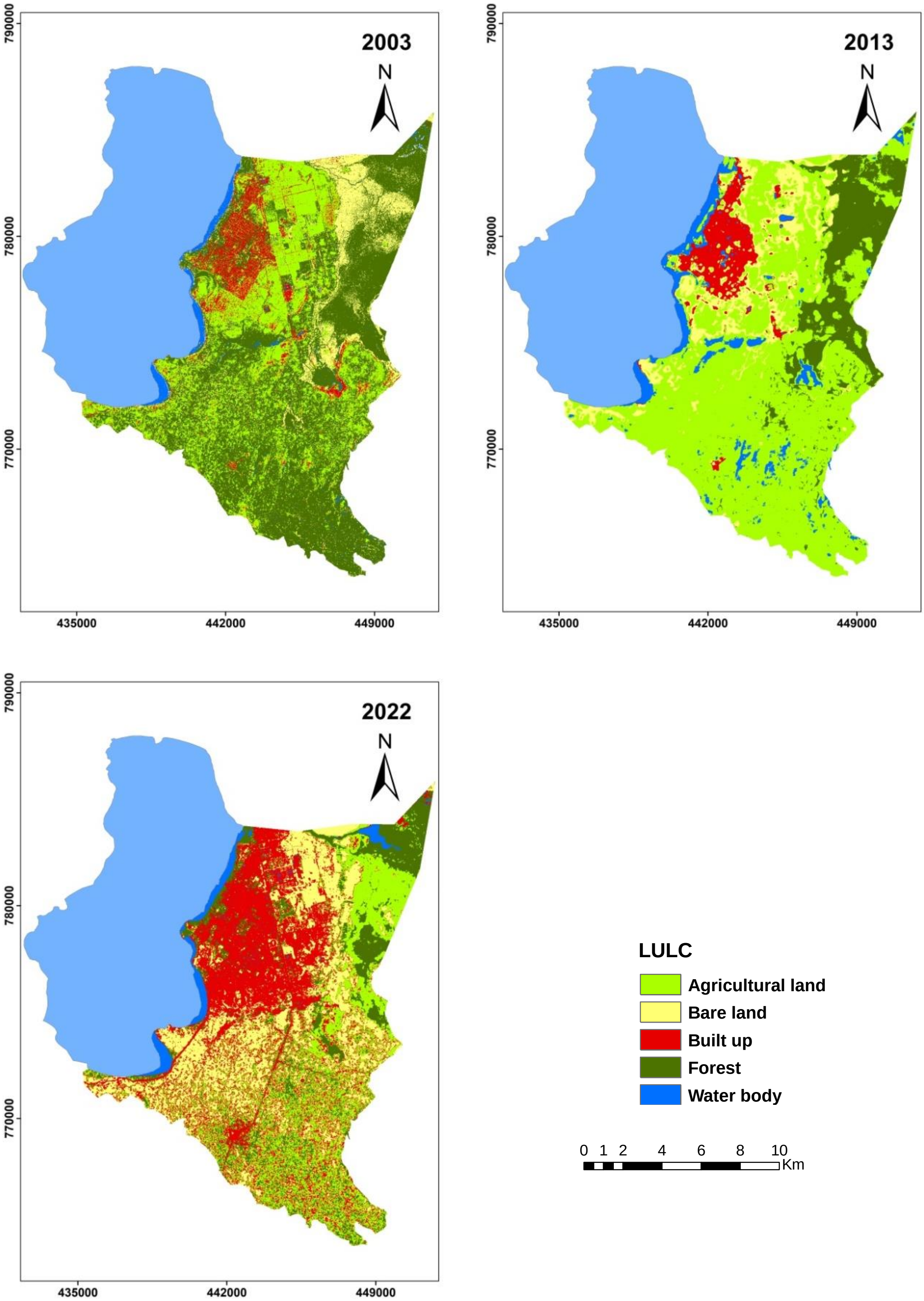

Fig 4.5 Land-use and land-cover of Hawassa

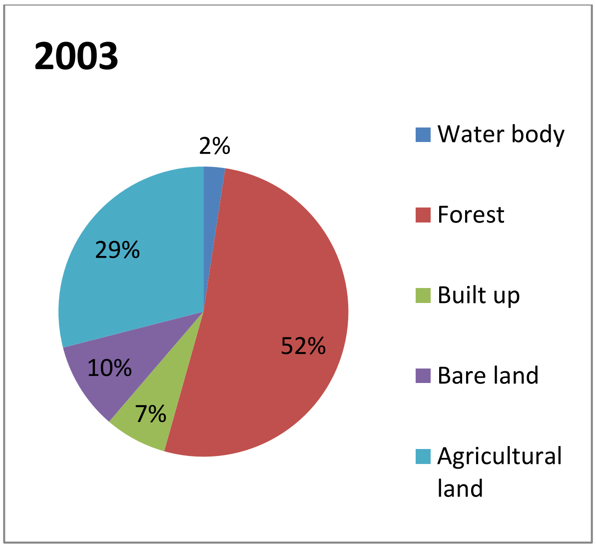

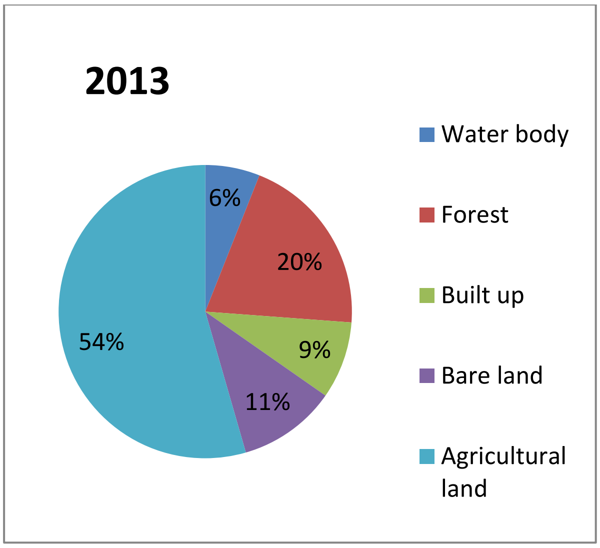

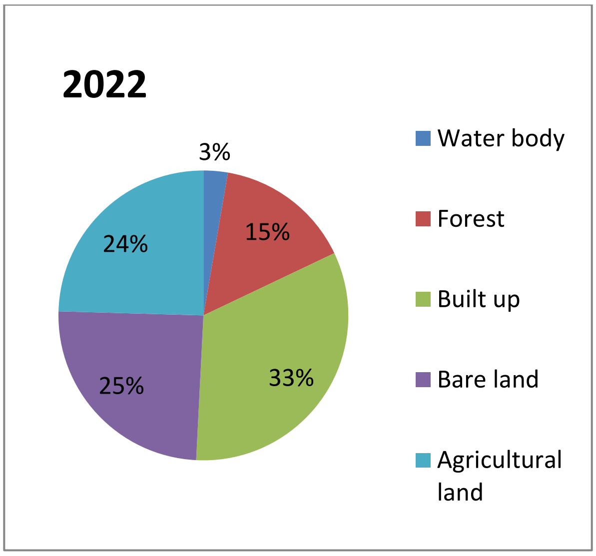

Fig 4.6 Pie-chart of land-use and land-cover of Hawassa

4.2 Extent and trend of land-use and land-cover change

4.2.1 Extent and trend of land-use and land-cover change Addis Ababa city

In Addis Ababa between 2003, 2013 and 2017, the study area's patterns of land use and land cover saw major changes. Agricultural land, bare land, and built-up areas showed the most significant changes throughout the duration of the study's 19 years. The built-up area has grown between 2003 and 2022. By 2022, it have grown from 11693.43 ha (21.6%) in 2003 to 34766.1ha (64.6%). Bare land decreased between 2003 and 2022. 2318.98 ha(4.3%) in 2022, down from 13562.14ha (25.1%) in 2003. From 2003 to 2022, agricultural land decreased as well. 10037.04ha (18.6%) in 2022, down from 22800.26ha

(42.2%) in 2003.From 2003 to 2013, a water body decreased by 0.57% while a forest increased by 2.1%.

Table 4.4 Net changes of land-use and land-cover of Addis Ababa during 2003-2022

LULC classes	2003-2013		2013-2022		2003-2022	
	(Area)Ha	(Area)%	(Area)Ha	(Area)%	(Area)Ha	(Area)%
Water body	-1694.54	-3.1	+1384.9	+2.56	-309.64	-0.57
Forest	+1215.08	+2.2	-63.41	-0.11	+1151.67	+2.1
Built up	+10614.51	+19.6	+12458.16	+23.1	+23072.67	+42.7
Bare land	-2533.95	-4.7	-8709.02	-16.1	-11243.16	-20.8
Agricultural land	-7513.92	-13.9	-5249.3	-9.7	-12763.22	-23.6

4.2.2 Extent and trend of land-use and land-cover change Adama city

Between 2003, 2013, and 2022, there were significant changes in Adama's land use and land cover patterns. The three types of classes that underwent the most changes during the duration of the 19-year research were agricultural land, bare land, and built-up regions. From 2003 to 2022, the built-up area increased by 2620.48ha (23.8%). Additionally, bare land grew by 1547.49ha (14%) between 2003 and 2022. Agriculture land decreased by 4701.17ha (42.8%) between 2003 and 2022. The amount of water and forest increased by 1.2% and 3.3%, respectively, between 2003 and 2022.

Table 4.5 Net changes of land-use and land-cover of Adama during 2003-2022

LULC classes	2003-2013		2013-2022		2003-2022	
	(Area)Ha	(Area)%	(Area)Ha	(Area)%	(Area)Ha	(Area)%
Water body	-117.09	-1.0	+250.25	+2.3	+133.16	+1.2
Forest	+33.01	+0.3	+328.84	+3.0	+361.85	+3.3
Built up	+311.78	+2.8	+2308.7	+21	+2620.48	+23.8
Bare land	+1262	+11.5	+285.49	+2.6	+1547.49	+14
Agricultural land	-1481.83	-13.5	-3219.34	-3.0	-4701.17	-42.8

4.2.3 Extent and trend of land-use and land-cover change Hawassa city

The study area's patterns of land use and land cover saw significant changes in Hawassa between 2003, 2013, and 2022. Over the course of the 19-year study, the most notable changes were observed in built-up areas, bare land, and agricultural land. The area that has been built up expanded by 4306.86 ha (25.7%) between 2003 and 2022. Between 2003 and 2022, the amount of bare land increased by 2482.77ha (14.8%). A reduction of 741.81ha (4.4%) in agricultural land has been showen between 2003 and 2022. The amount of water increased slightly between 2003 and 2022, whereas the area of forest decreased by 3.6%.

Table 4.6 Net changes of land-use and land-cover of Hawassa during 2003-2022

LULC classes	2003-2013		2013-2022		2003-2022	
	(Area)Ha	(Area)%	(Area)Ha	(Area)%	(Area)Ha	(Area)%
Water body	+595.41	+3.5	-548.75	-3.2	+46.66	+0.27
Forest	-5275.46	-31.3	-838.78	-5	-6114.24	-3.6
Built up	+268.98	+1.6	+4037.88	+24	+4306.86	+25.7
Bare land	+181.26	+1.0	+2301.51	+13.7	+2482.77	+14.8
Agricultural land	+4267.86	+25	-5009.67	-30	-741.81	-4.4

4.3 Accuracy Assessment

Because classified land cover maps from remotely sensed images contain various types of errors, it is the responsibility of the researcher to find out those errors so as to make the produced land cover maps become reliable and easily interpretable by users. Once the classified image is integrated into a GIS, to become an information source for urban planners and researchers, accuracy assessment should be processed as it limits the classification results of a remotely sensed imagery data. To do so, the accuracy of a classified map has to be assessed and compared with a referenced data using an error matrix as explained in chapter 3 of section 3.6.3. The accuracy assessment in this study is given in the table 4.7.

Table 4.7 Statistical information of accuracy assessment

Cities	Overall accuracy (%)			Overall Kappa(K) statistics		
	2003	2013	2022	2003	2013	2022
Addis Ababa	80	76	85	0.74	0.61	0.8
Adama	79	78	81	0.72	0.71	0.76
Hawassa	77	75	82	0.7	0.67	0.76

4.4 Normalized Difference Vegetation Index (NDVI)

4.4.1 Addis Ababa normalized difference vegetation index

The study area's estimated surface vegetation intensity and distribution pattern using the normalized vegetation index demonstrate that the red color has a comparatively low NDVI value while the green color shows a high NDVI value. Each study year's NDVI value was different. The study found that the year 2003's maximum NDVI value is higher than that of 2013 and 2022. The study's area's upper part, where there is more vegetation than in other parts, has the highest NDVI value, while the center and south-east regions of the study, where there is more built-up area, have the lowest values. The maximum and minimum NDVI value of the study years are -0.36 to 0.66, -0.24 to 0.49 and -0.15 to 0.59 for the year 2003, 2013 and 2022 respectively. Figure 4.7 shows the NDVI map of the study area.

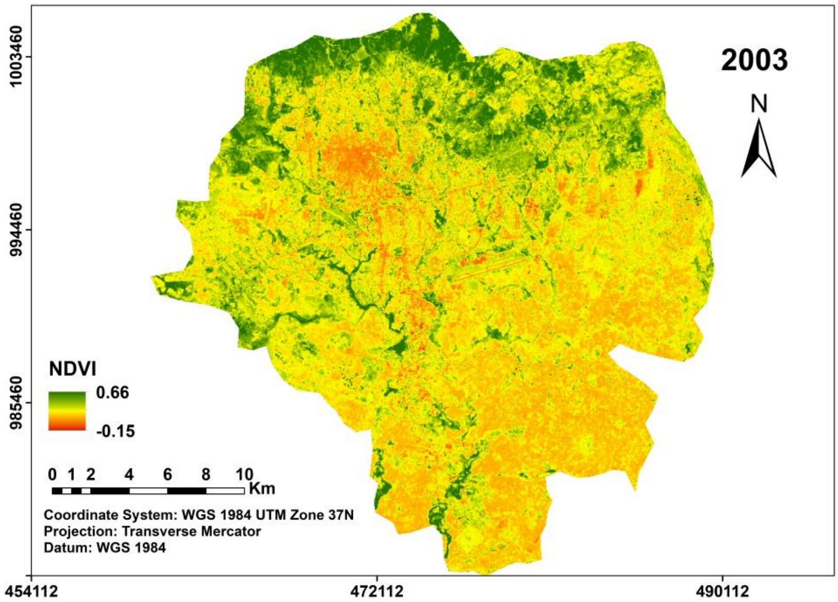

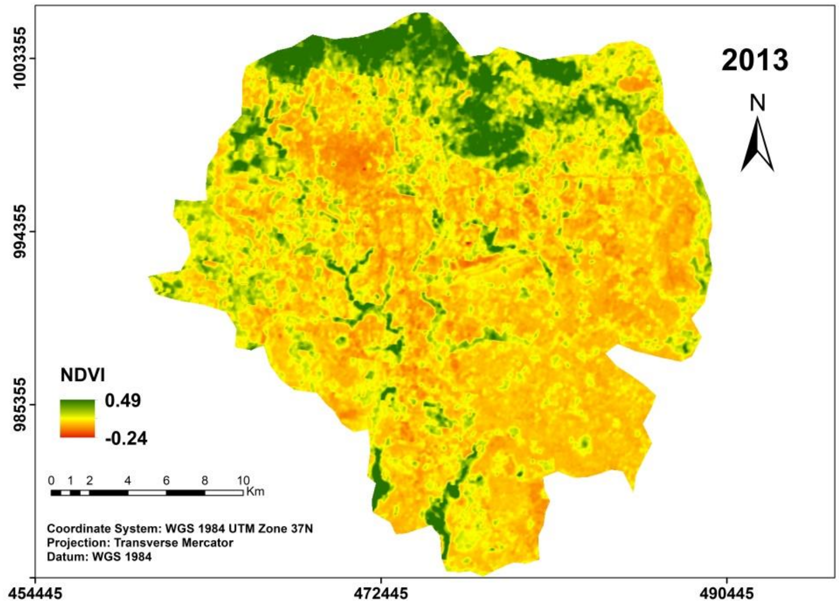

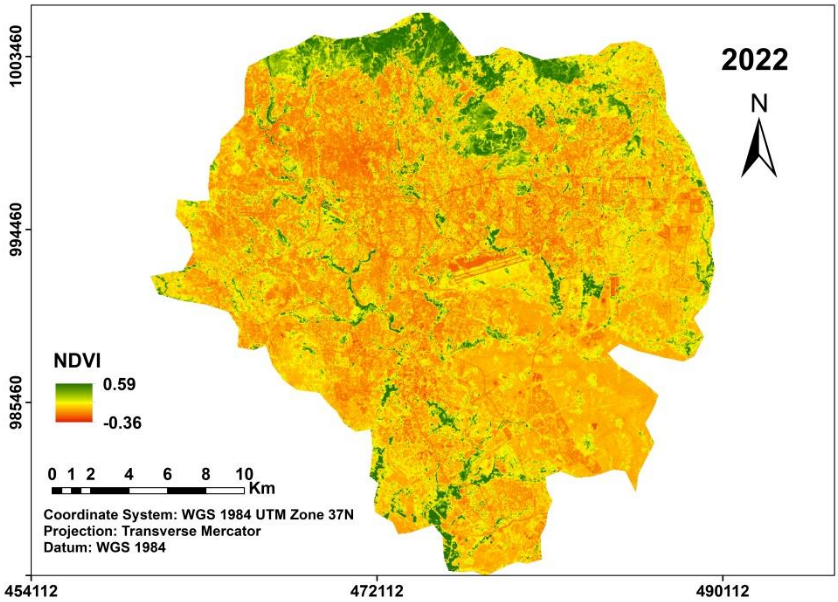

Fig 4.7 NDVI maps of Addis Ababa city

4.4.2 Adama normalized difference vegetation index

The normalized vegetation index was used to estimate the surface vegetation intensity and distribution pattern in the study area, and the results show that red has a relatively low NDVI value while green has a high NDVI value. The value of the NDVI varies depending on the study's year. The highest NDVI value for the study year 2003 is higher than it is for 2013 and 2022. The southern part of the study area, which has higher vegetation cover than the other regions, has the highest NDVI value. Due to built-up areas, low NDVI values were observed in the study area's central and northwest parts. The study years' maximum and minimum NDVI values are, respectively, -0.37 to 0.62, -0.1 to 0.37, and -0.17 to 0.52 for the years 2003, 2013, and 2022. Figure 4.8 shows the NDVI map of the study area.

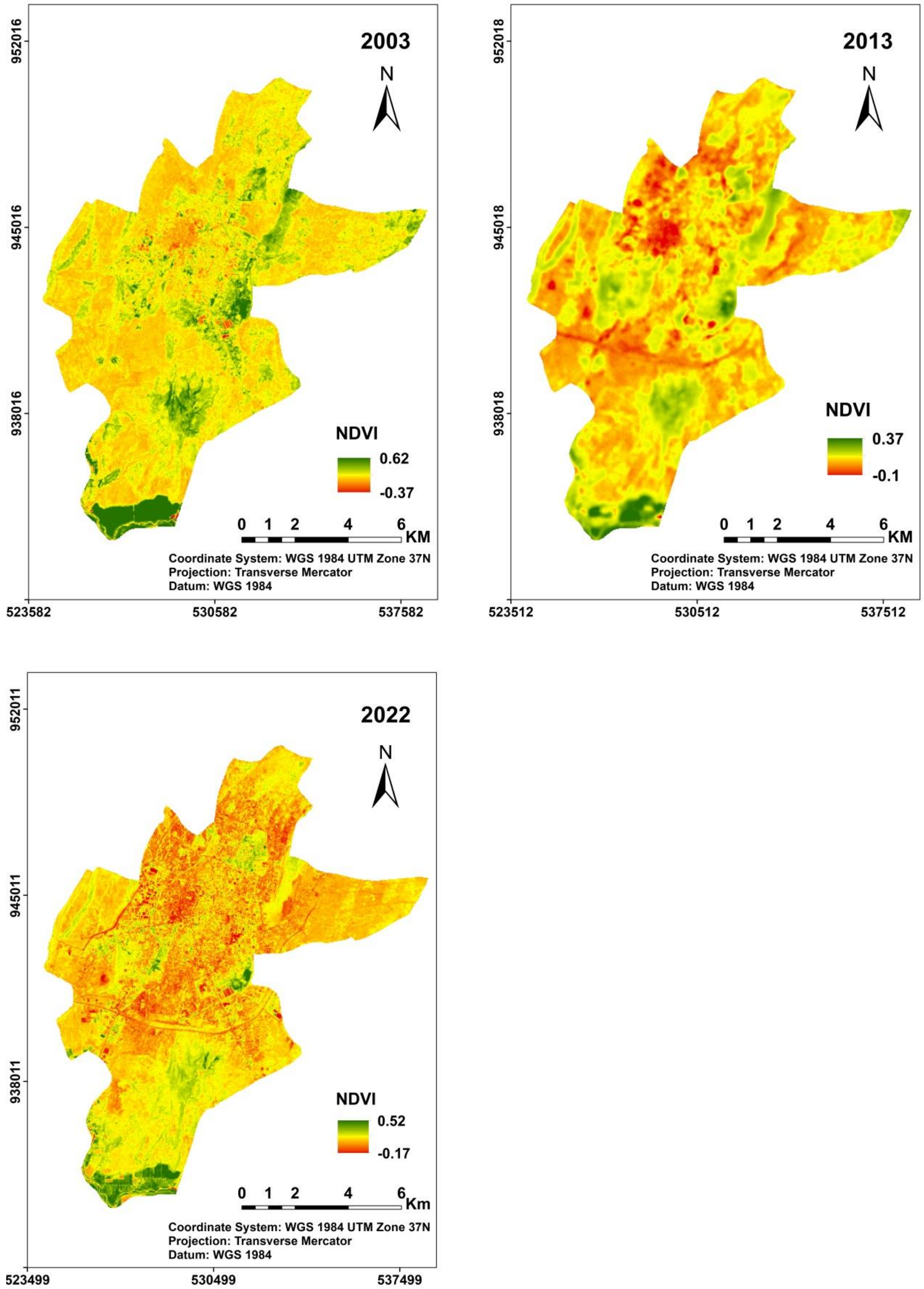

Fig 4.8 NDVI maps of Adama city

4.4.3 Hawassa normalized difference vegetation index

According to the normalized vegetation index's predicted surface vegetation intensity and distribution pattern for the research region, the red color has a relatively low NDVI value while the green color exhibits a high NDVI value. The value of the NDVI varies depending on the research year. The highest NDVI value for the research year 2003 is higher than it is for 2013 and 2022. The north-east of the study area, which has greater vegetation cover than the other areas, has the highest NDVI value. Due to built-up areas, the north-west of the study area had the lowest NDVI value. The study years' maximum and minimum NDVI values are -0.28 to 0.6, -0.21 to 0.48, and -0.31 to 0.5 respectively. Figure 4.9 shows the NDVI map of the study area.

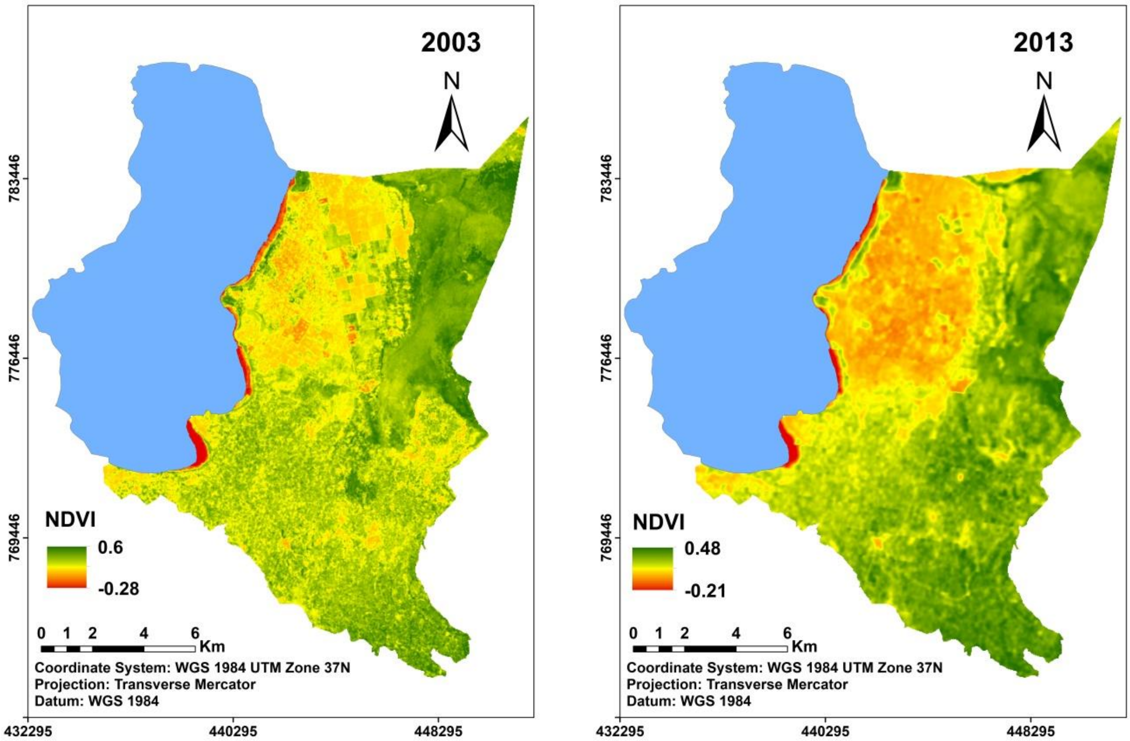

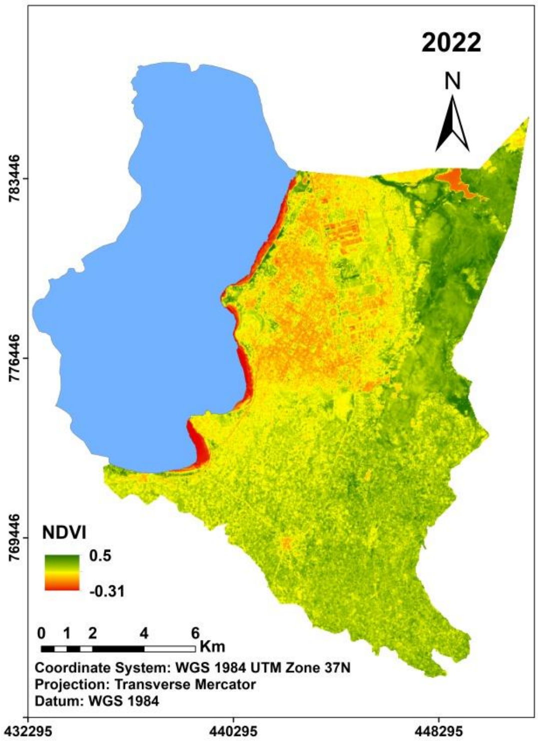

Fig 4.9 NDVI maps of Hawassa city

4.5 Normalized Difference Built-up Index

4.5.1 Addis Ababa normalized difference built-up index

According to the built-up index depicted in Figure 4.10, the positive values defining the area under built-up are strong. Built-up areas are shown by the areas under the red to yellow colours, and non- built up areas are shown by the areas under the green colours. The LST and temperature both rise as a result of the high reflection of surface features. The study's region's north-west, which has more built-up area than the other areas of the study area, has the highest NDBI value. Due to areas covered in vegetation, the upper part of the study area had the lowest NDBI value. The studied years' maximum and minimum NDBI values are -0.54 to 0.50, -0.41 to 0.30, and -0.44 to 0.6 for the years 2003, 2013, and 2022 respectively.

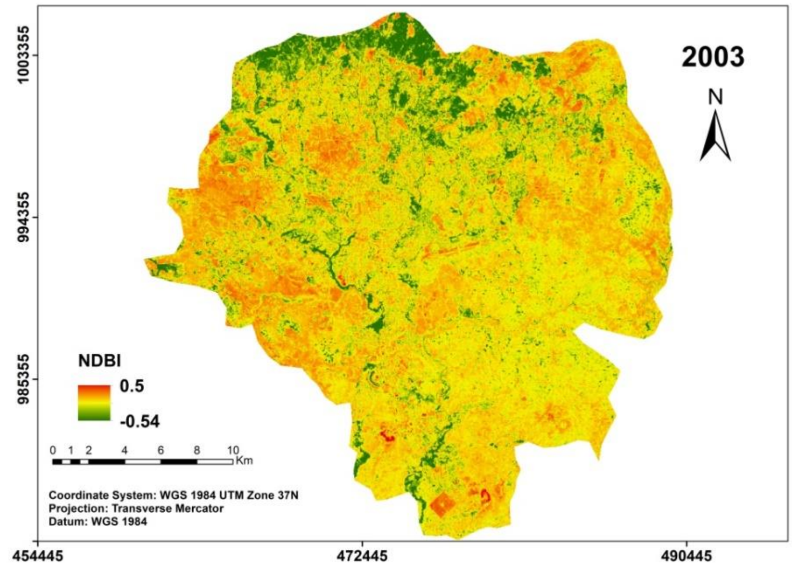
2003
N
NDBI
0.5
-0.54
0 1 2 4 6 8 10 Km
Coordinate System: WGS 1984 UTM Zone 37N
Projection: Transverse Mercator
Datum: WGS 1984
1003355
994355
985355
454445
472445
490445

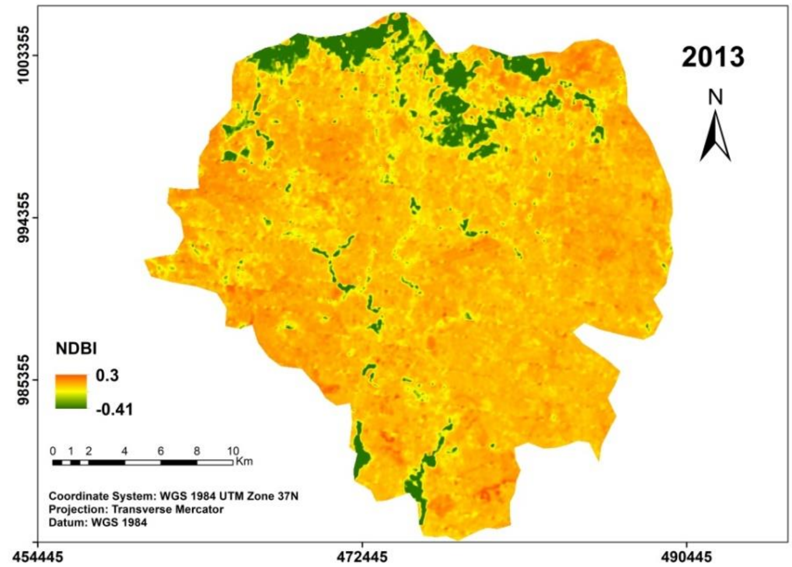
2013
N
NDBI
0.3
-0.41
0 1 2 4 6 8 10 Km
Coordinate System: WGS 1984 UTM Zone 37N
Projection: Transverse Mercator
Datum: WGS 1984
1003355
994355
985355
454445
472445
490445

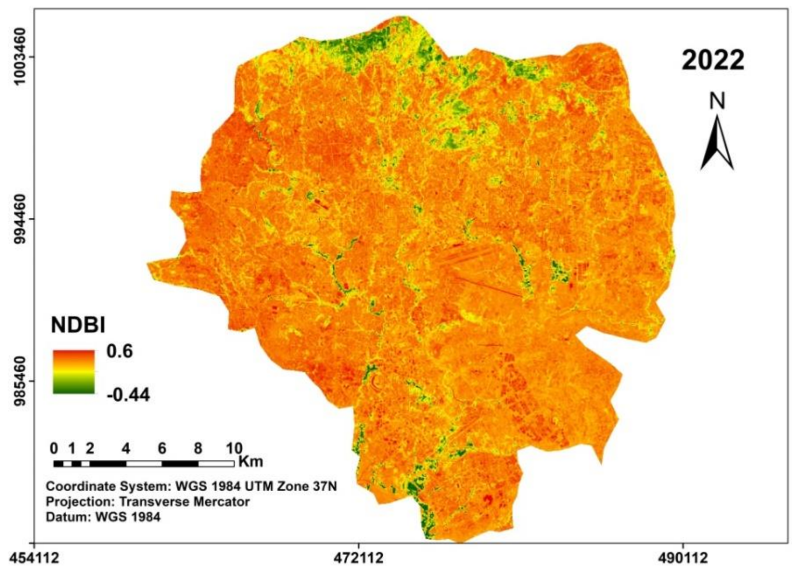
2022
N
NDBI
0.6
-0.44
0 1 2 4 6 8 10 Km
Coordinate System: WGS 1984 UTM Zone 37N
Projection: Transverse Mercator
Datum: WGS 1984
1003460
994460
985460
454112
472112
490112

Fig 4.10 NDBI maps of Addis Ababa city

4.5.2 Adama normalized difference built-up index

The positive values indicating the area under built-up and bare land are strongly defined by the built-up index shown in Figure 4.11. Due to their spectral proximity of built-up and bare land areas, they have high NDBI value. They are represented by the areas under the red to yellow colors, whereas the areas under the green colors represent non-built up lands. The high reflection of surface features causes a rise in both the LST and temperature. The maximum and minimum NDBI values for the evaluated years are, respectively, -0.55 to 0.37, -0.29 to 0.28, and -0.35 to 0.41 for the years 2003, 2013, and 2022.

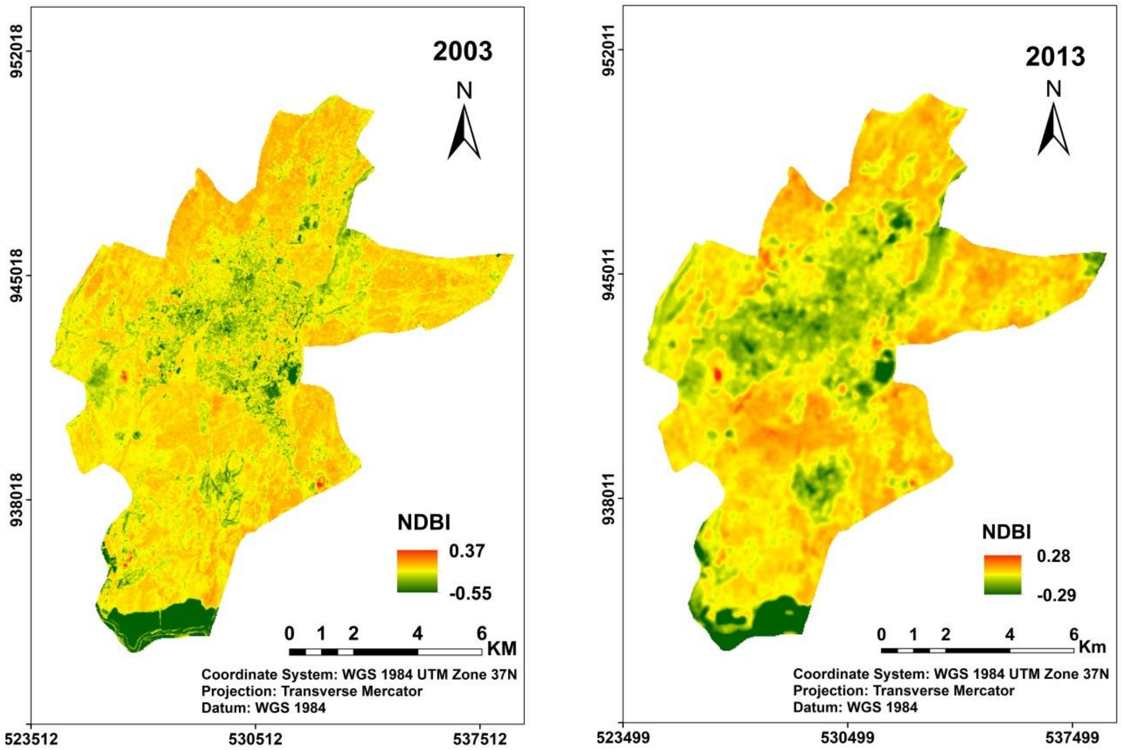

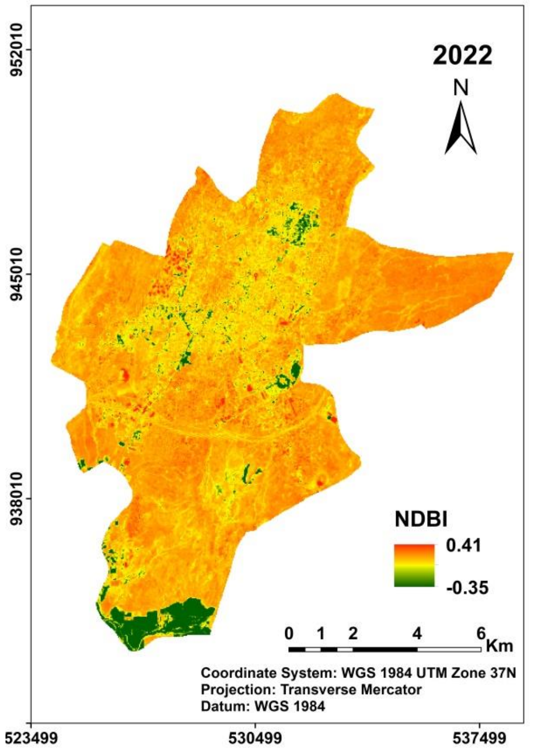

Fig 4.11 NDBI maps of Adama city

4.5.3 Hawassa normalized difference built-up index

The area under built-up is strongly defined by positive values, according to the built-up index shown in Figure 4.12. Due to their spectral proximity of built-up and bare land areas, they have high NDBI value. Areas under the red to yellow colors indicate built-up and bare land areas, whereas areas under the green colors indicate non-built up areas. The high reflection of surface features causes a rise in both the LST and temperature. The north-west of the study area, which is more densely populated than the other parts, has the highest NDBI value. The north-east portion of the study area had the lowest NDBI value because of vegetation cover. Maximum and minimum NDBI values for the examined years are -0.54 to 0.32, -0.35 to 0.25, and -0.35 to 0.39 for the years 2003, 2013 and 2022 respectively.

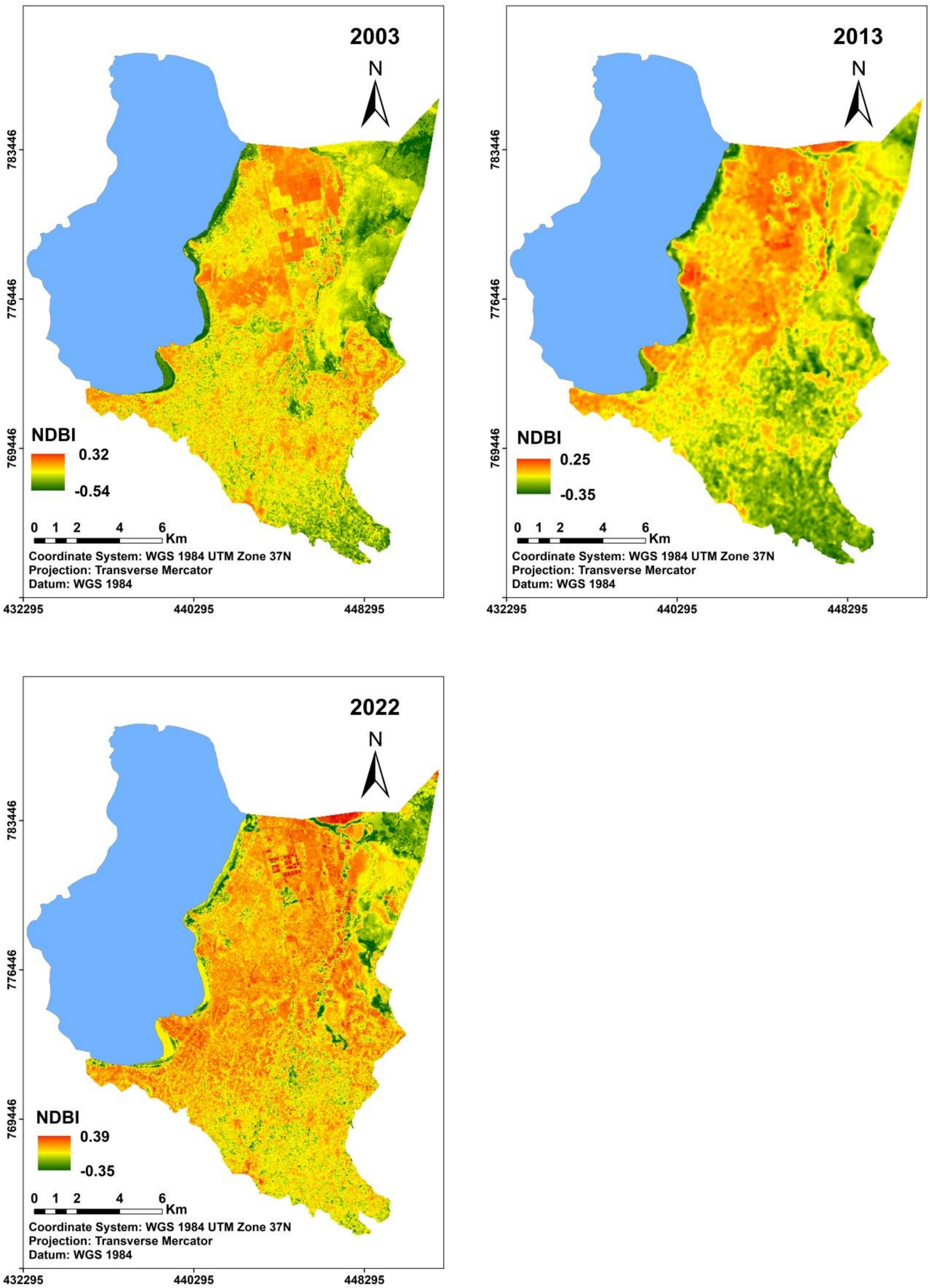

Fig 4.12 NDBI maps of Hawassa city

4.6 Land Surface Temperature

4.6.1 Addis Ababa land surface temperature

Using ASTER's night time thermal bands, the spatial distribution of LST in the study area was retrieved and quantified; the deep orange colour showed the highest land surface temperature of the study area whereas the green is the lowest land surface temperature of the study area. According to analysis of these images, the study period's LST values for 2002 ranged from -3.96°C to 14.52°C and for 2022 from -2.47°C to 17.16°C with mean temperature of 9.13°C and 12.19°C. The center, south, and some east parts of the study area showed relatively high temperatures, as could be seen from the thermal images that had been analyzed. The main causes of this include altitude, slope, and LULC types. However, the LST values were rather low in the northern part of study area. Figure 4.13 shows the LST map of the study area.

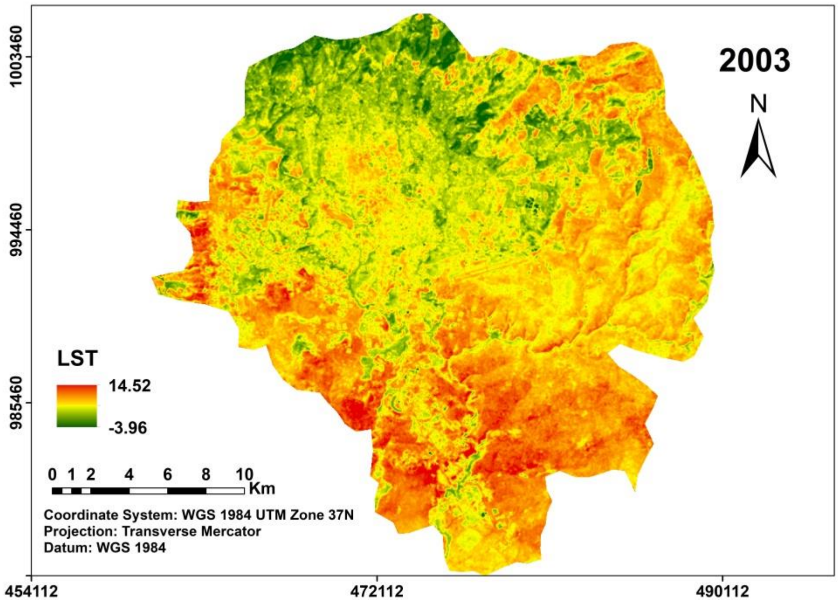

i5

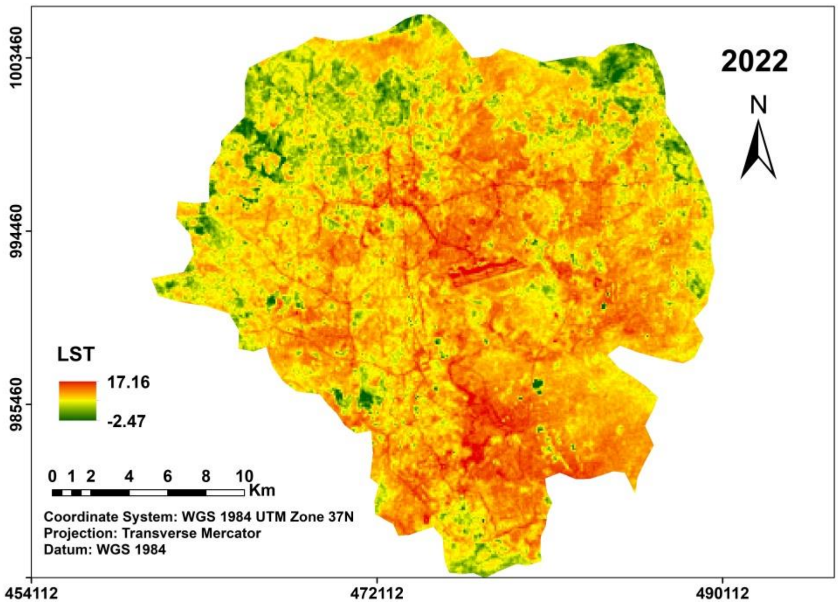

Fig 4.13 LST maps of Addis Ababa city

4.6.2 Adama land surface temperature

The spatial distribution of LST of the study area was retrieved and quantified using ASTER night time thermal bands for the years 2003, 2013, and 2022; the deep orange colour showed the highest land surface temperature of the study area, and the green is the lowest land surface temperature of the study area. According to the study of these images, the LST value for the study period ranged from 11.2°C to 21.3°C, 12.61°C to 24.38°C, and 13.11°C to 24.93°C, whereas the mean temperature for the study area was 17.63°C, 20.91°C, and 21.97°C in 2003, 2013, and 2022, respectively. Temperature changes across places are mostly caused by altitude, slope, and LULC types. Figure 4.14 depicts the study area's LST map.

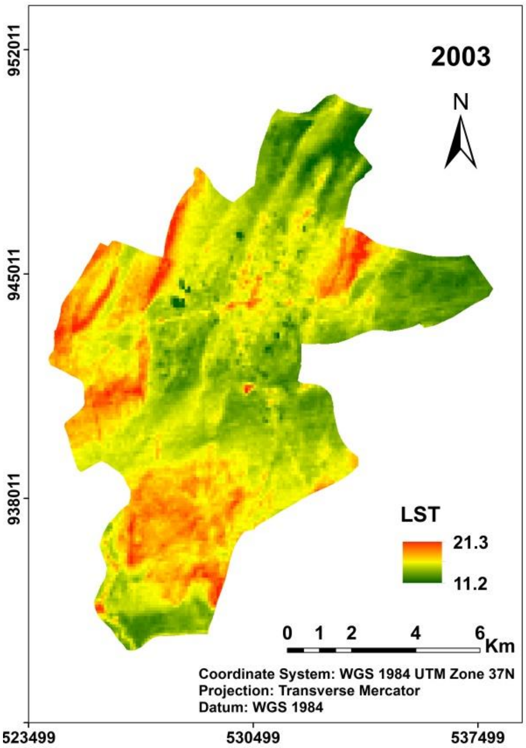

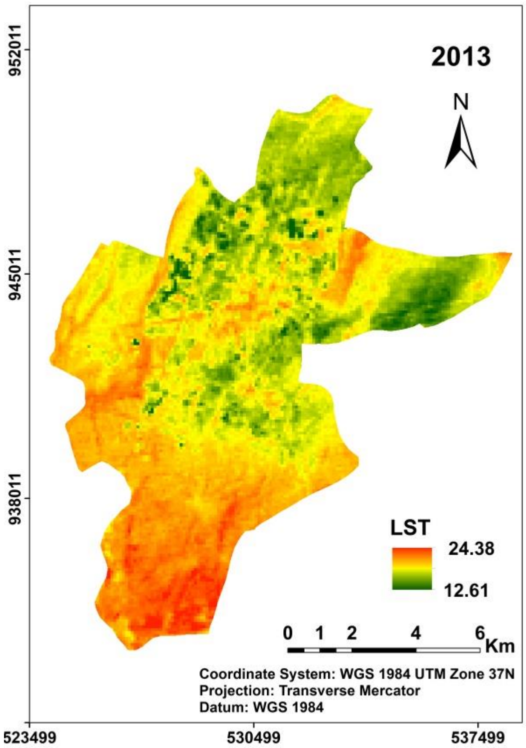

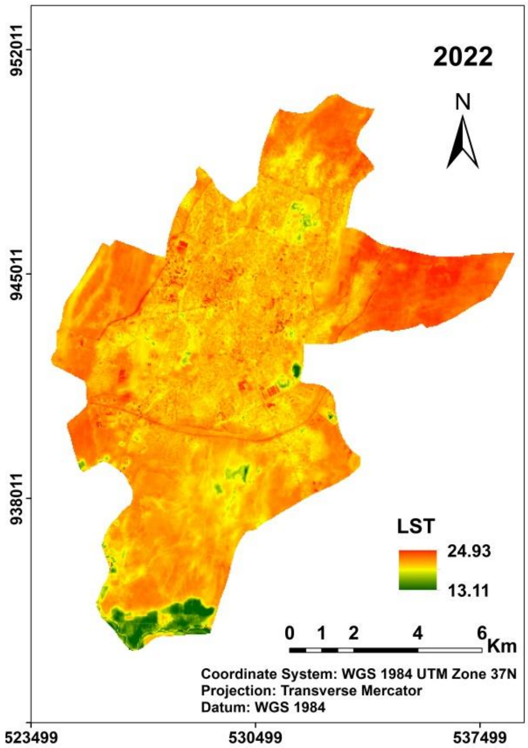

Fig 4.14 LST maps of Adama city

4.6.3 Hawassa land surface temperature

The spatial distribution of LST in the study area was retrieved and quantified using ASTER night time thermal bands for the years 2003, 2013, and 2022; the deep orange colour indicated the study area's highest land surface temperature, while the green colour indicated its lowest. The examination of these images showed that the LST value for the study's time period was between 8.02°C and 21.49°C, 11.07°C and 24.38°C, and 13.82°C and 24.71°C, respectively, while the mean temperature for the study area was 12.80°C, 16.47°C, and 17.60°C in 2003, 2013, and 2022, respectively. Changes in temperature throughout a region are mostly caused by altitude, slope, and LULC types. The LST map of the research region is displayed in Figure 4.15.

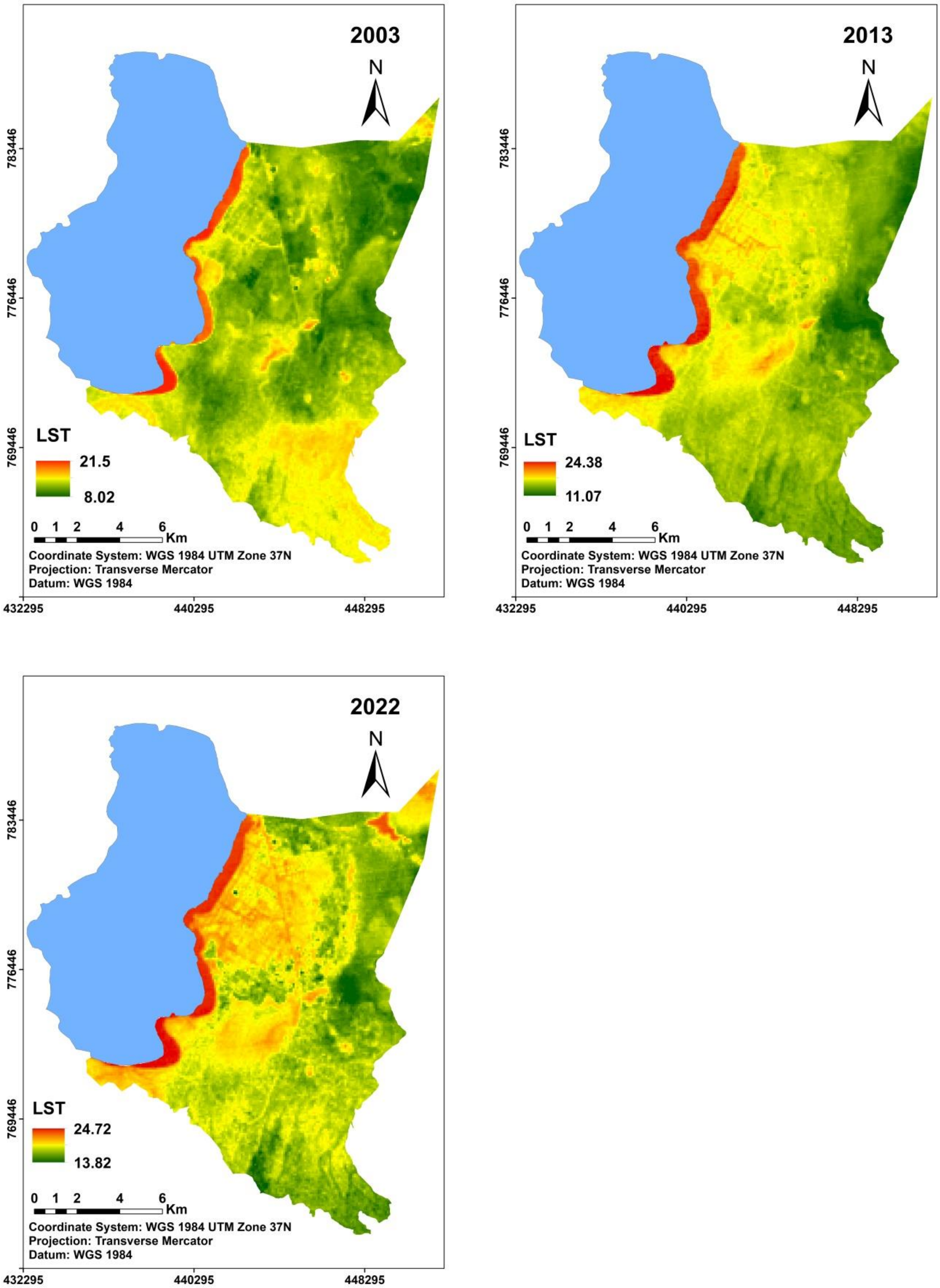

Fig 4.15 LST maps of Hawassa city

4.7 Relationship between land-use and land-cover types with land surface temperature

4.7.1 Zonal statistics of LULC with LST

Addis Ababa land-use and land-cover types and LST map showed how the categories' corresponding land surface temperatures changed during the period of the study. The types of land-use and land-cover that recorded the lowest temperatures were forest and agricultural land. In the years 2002 and 2022, the mean land surface temperatures of agricultural and forested land, respectively, were 8.23 °C and 8.42 °C and 11.89 °C and 11.94 °C. And the areas with the highest temperatures were bare land, built-up areas, and water bodies. In 2002, the mean land surface temperatures of water bodies, built-up areas, and bare land were 9.12 °C, 9.04 °C, and 8.76 °C, respectively. By 2022, same values would be 12.26 °C, 15.13 °C, and 14.09 °C (Table 4.8).

Table 4.8 Zonal statistic of LULC and LST for Addis Ababa

LULC	**2002**			**2022**		
	Min(°C)	Max(°C)	Mean(°C)	Min(°C)	Max(°C)	Mean(°C)
Water	3.96	13.43	9.12	5.48	17.16	12.26
Forest	2.03	12.94	8.23	6.39	17.11	11.89
Built up	-3.73	14.47	9.04	-2.47	17.16	15.13
Bare Land	3.21	13.72	8.76	7.13	16.44	14.09
Agricultural land	-3.42	14.13	8.42	-2.47	17.16	11.94

The LST map and Adama land-use and land-cover types displayed changes in the appropriate categories' land surface temperatures during the course of the study. The mean temperature in the forest was 17.72 °C in 2003, 20.44 °C in 2013, and 22.12 °C in 2022, respectively. For agricultural land, 17.54°C, 20.79°C, and 22.34°C. Water bodies are at 17.69°C, 21.56°C, and 21.75°C.For built-up, 17.67°C, 20.39°C, and 22.72°C. For the three years of study, bare land had temperatures of 18.10°C, 21.14°C, and 23.22°C (Table 4.9).

Table 4.9 Zonal statistic of LULC and LST for Adama

LULC	2003(°C)			2013(°C)			2022(°C)		
	Min	Max	Mean	Min	Max	Mean	Min	Max	Mean
Water	12.58	20.81	17.69	16.14	23.84	21.56	16.25	23.87	21.75
Forest	11.21	21.30	17.72	12.62	24.38	20.44	13.82	24.64	22.12
Built up	11.21	21.19	17.67	15.80	24.38	20.39	15.36	24.78	22.72
Bare Land	11.21	21.30	18.10	14.99	24.05	21.14	16.53	24.30	23.22
Agricultural land	11.21	21.30	17.54	12.62	24.38	20.79	12.98	24.12	22.34

The Hawassa land-use and land-cover types and LST map displayed changes in the relevant land surface temperatures for every class across the study period. The mean temperature in the forest was 12.87 °C in 2003, 14.09 °C in 2013, and 17.68 °C in 2022, respectively. agricultural land: 12.79°C, 16.27°C, and 16.61°C. Water bodies are at 17.40°C, 19.64°C, and 22.61°C.For built-up, 13.05°C, 18.69°C, and 21.98°C. For bare land, temperatures of 11.45°C, 17.79°C, and 20.48°C were noted for each of the study's three years (Table 4.10).

Table 4.10 Zonal statistic of LULC and LST for Hawassa

LULC	2003(°C)			2013(°C)			2022(°C)		
	Min	Max	Mean	Min	Max	Mean	Min	Max	Mean
Water	8.43	21.50	17.40	12.24	24.38	19.64	14.87	24.43	22.61
Forest	8.02	21.45	12.87	10.11	23.96	14.09	12.23	24.72	17.68
Built up	8.30	21.32	13.05	13.87	24.10	18.69	12.15	24.72	21.98
Bare Land	8.05	21.32	11.45	10.17	24.10	17.79	12.15	24.64	21.48
Agricultural land	8.02	21.32	12.79	9.82	24.38	16.27	12.15	24.72	16.61

4.7.2 Changes in temperature during 2003−2022 in the study area

The mean LST in Addis Ababa has increased by 3.06 °C between 2002 and 2022. According to Table 4.11, the LST increased across the board for all significant LULC categories during the study period. Built-up and bare land areas had the largest mean LST change. The forest area had the lowest mean change LST, though. Figure 4.16 shows comparisons of mean LST with LULC classes over the study period. From 2002 to 2022, the land surface temperature in the study area increased significantly.

Table 4.11 Mean change in temperature during 2003−2022 in Addis Ababa

LULC	2003-2022
	Mean change(°C)
Water	3.14
Forest	2.66
Built up	6.09
Bare Land	5.33
Agricultural land	3.52

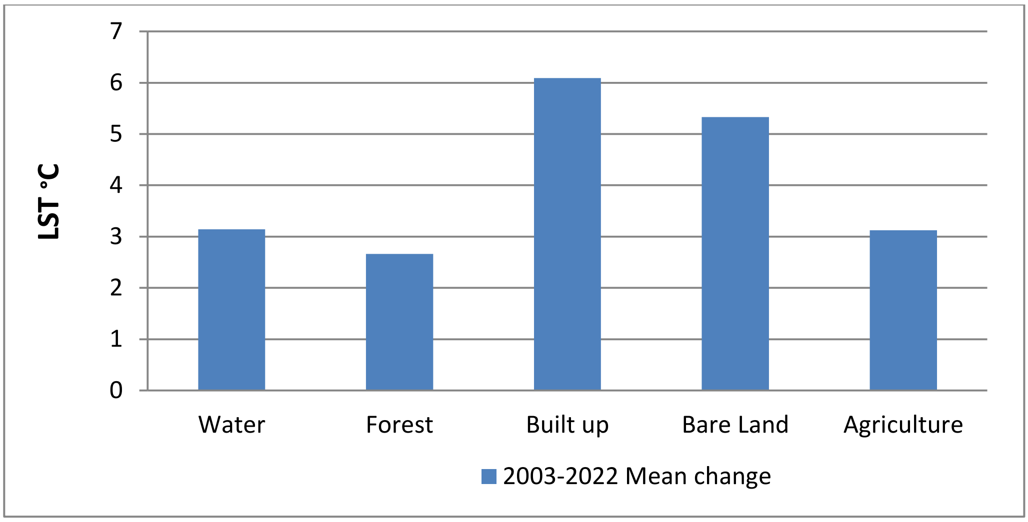

Fig 4.16 Comparisons of mean LST in different LULCC for Addis Ababa

Between 2003 and 2022, Adama's mean LST increased by 4.34 °C. Table 4.12 shows that over the study's period, the LST increased uniformly for all significant LULC classes. The highest mean LST change was seen in built-up and bare land areas. On the other side, the water body experienced the lowest mean change in LST. Comparisons of mean LST with LULC classes over the research period are shown in Figure 4.17. The study area's land surface temperature increased significantly between 2003 and 2022.

Table 4.12 Mean change in temperature during 2003-2022 in Adama

LULC	2003-2013 Mean change(°C)	2013-2022 Mean change(°C)	2003-2022 Mean change(°C)
Water	3.87	0.19	4.06
Forest	2.72	1.68	4.4
Built up	3.72	2.33	5.05
Bare Land	3.04	2.08	5.12
Agricultural land	3.25	1.55	4.8

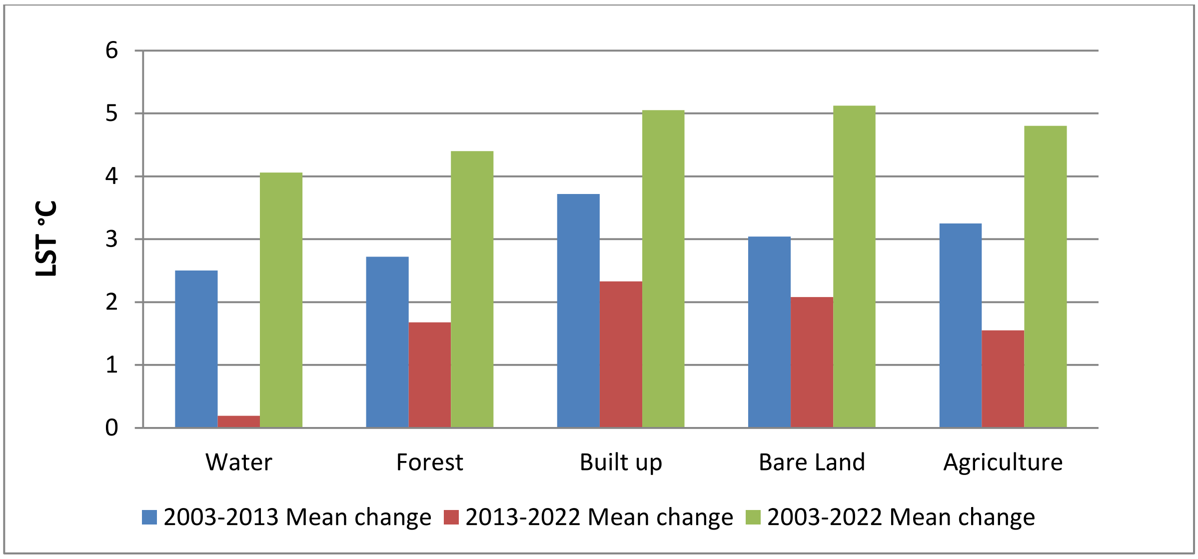

Fig 4.17 Comparisons of mean LST in different LULCC for Adama city

Hawassa's mean LST increased by 4.8 °C between 2003 and 2022. In all important LULC classes over the study's period, the LST increased, as shown in Table 4.13. The highest mean LST change was in built-up and bare land areas. Contrarily, the mean LST change in agricultural land was the lowest. The mean LST and LULC classes for the study period are compared in Figure 4.18. In the study area, there was a considerable increase in land surface temperature between 2003 and 2022.

Table 4.13 Mean change in temperature during 2003-2022 in Hawassa

LULC	2003-2013	2013-2022	2003-2022
	Mean change(°C)	Mean change(°C)	Mean change(°C)
Water	2.24	2.97	5.21
Forest	1.22	3.59	4.81
Built up	5.64	3.29	8.93
Bare Land	6.34	2.69	9.03
Agricultural land	3.48	0.34	3.82

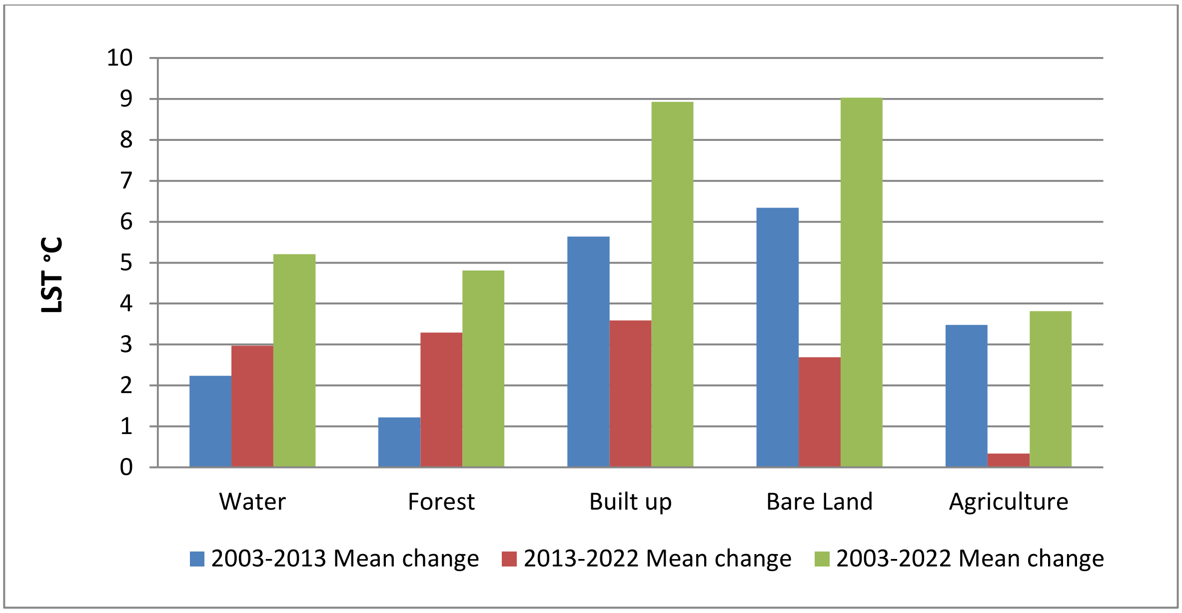

Fig 4.18 Comparisons of mean LST in different LULCC for Hawassa city

4.8 Relationship between normalized difference vegetation index with normalized difference built-up index

4.8.1 Relationship between normalized difference vegetation index with normalized difference built-up index of Addis Ababa city

According to the examined images from 2003 and 2022, there are indirect (inverse) correlations between NDVI and NDBI. High NDBI is associated with low NDVI levels, and vice versa. The NDVI and NDBI correlations' R^2 values throughout the study period were 77.57% and 62.41%, respectively. These findings demonstrate that in 2003, 77.57% of NDBI variability was caused by variations in NDVI values, and that in 2022, the coefficient variation values will likewise be the same. In general, there was a negative correlation between NDVI and NDBI values. Figure 4.19 displays NDBI and NDVI a relationship for the years 2003 and 2022.

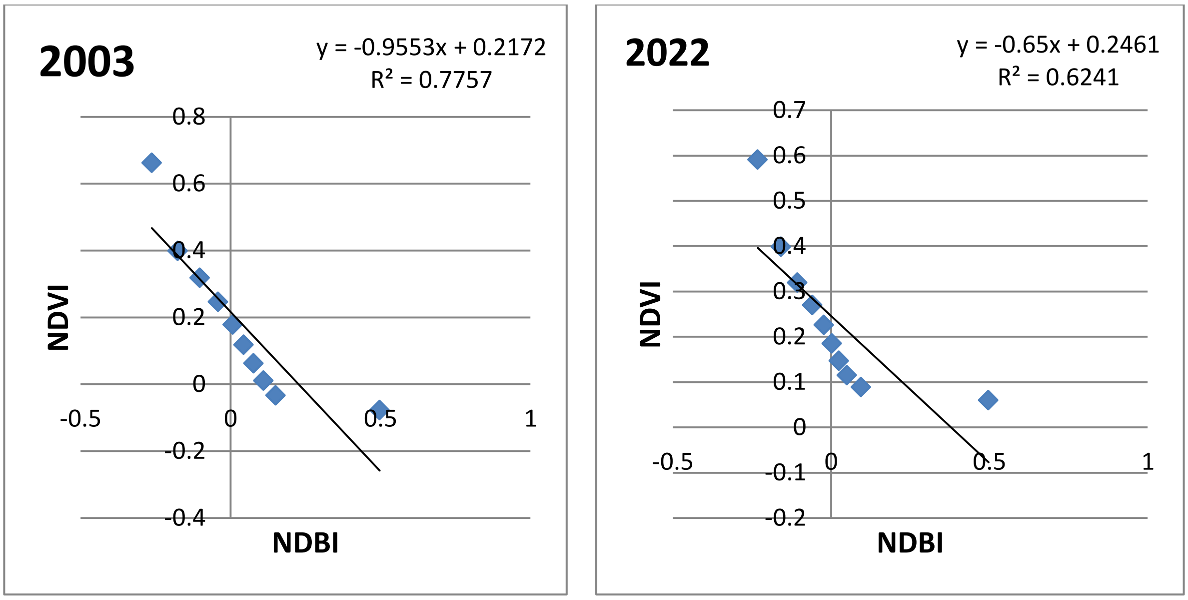

Fig 4.19 NDVI and NDBI correlation for Addis Ababa city

4.8.2 Relationship between Normalized Difference Vegetation Index with Normalized Difference Built-up Index of Adama city

The studied images from 2003, 2013, and 2022 show indirect (inverse) correlations between NDVI and NDBI. High NDBI and low NDVI levels are related to one another. The R^2values for the NDVI and NDBI correlations during the course of the study were 93.59%, 91.22%, and 77.27%, respectively. The results presented indicate that in 2003, as well as in 2013 and 2022, changes in NDVI values accounted for 93.59% of LST variability. In general, there was a negative correlation between NDVI and NDBI results. Figure 4.20 shows the correlation between NDBI and NDVI for the years 2003, 2013, and 2022.

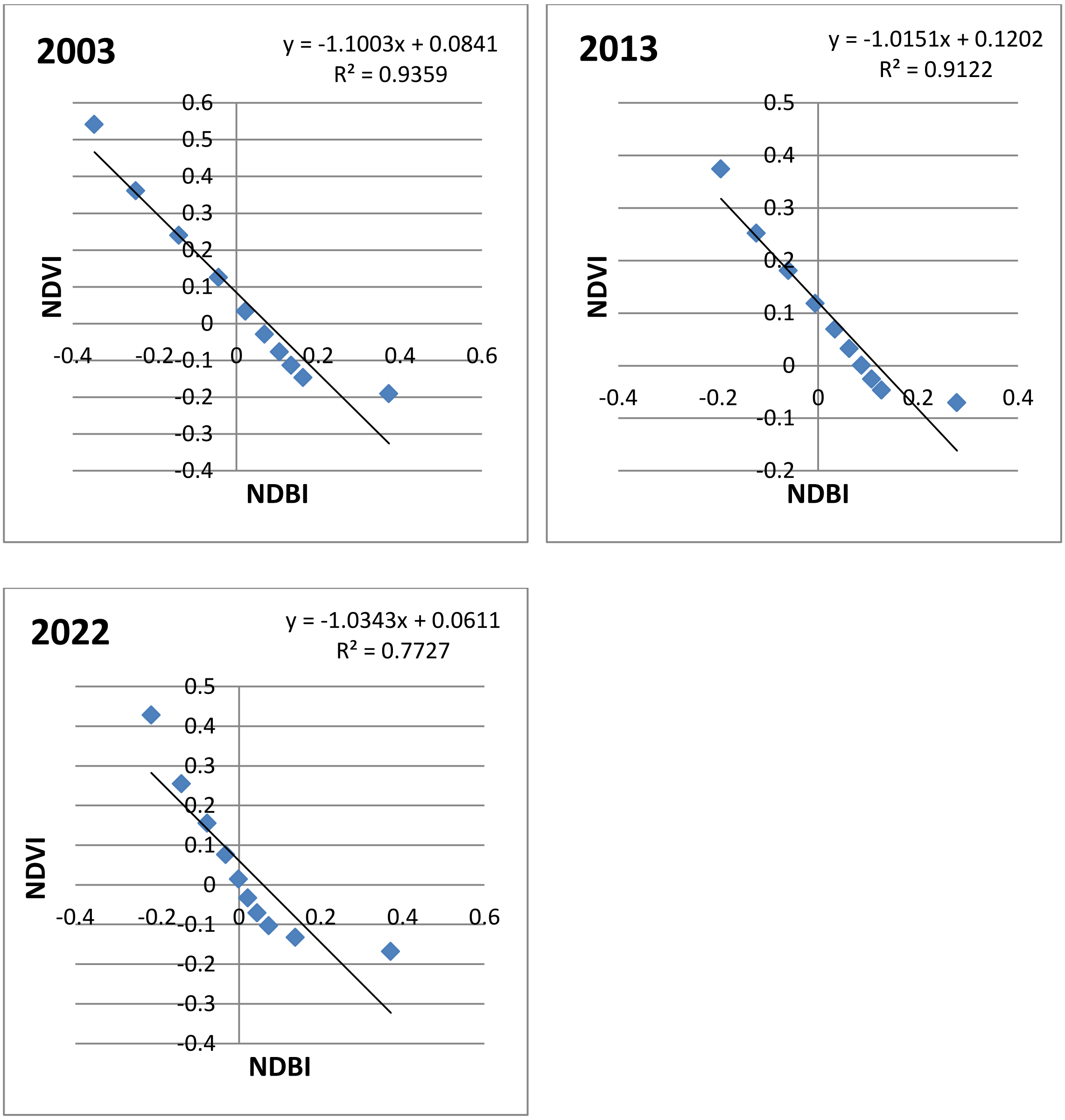

Fig 4.20 NDVI and NDBI correlation for Adama city

4.8.3 Relationship between normalized difference vegetation index with normalized difference built-up index of Hawassa city

There are indirect (inverse) relationships between NDVI and NDBI, according to the examined images from 2003, 2013, and 2022. Low NDVI values are related to high NDBI, and vice versa. Over the period of the study, the R^2 values for the NDVI and NDBI correlations were 95.64 %, 97.25 %, and 86.23 %, respectively. These results show that in 2003, variations in NDVI values accounted for 95.64 % of LST variability, and that in 2013 and 2022. NDVI and NDBI values generally had negative correlations with one another. The relationship between NDBI and NDVI for the years 2003, 2013, and 2022 is shown in Figure 4.21.

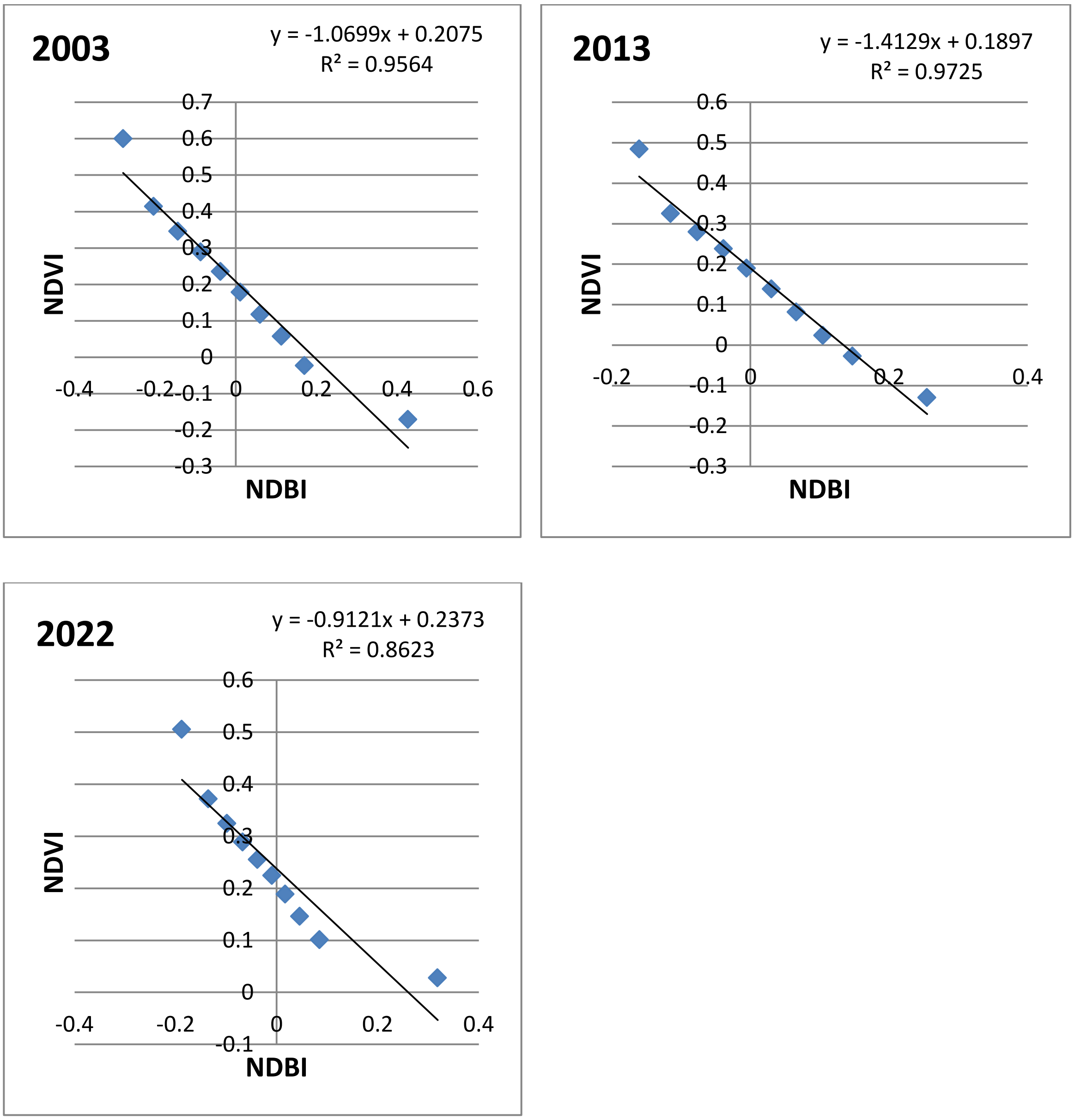

Fig 4.21 NDVI and NDBI correlation for Hawassa city

4.9 Relationship between normalized difference built- up index with land surface temperature

4.9.1 Relationship between normalized difference built- up index with land surface temperature of Addis Ababa city

According to the examined images from 2003 and 2022, there are direct correlations between NDBI and LST. High LST is associated with high NDBI levels, and low LST with low NDBI. The NDBI and LST correlations' R^2 values throughout the study period were 83.1 % and 89.15 %, respectively. These findings demonstrate that in 2003, 83.1 %

of LST variability was caused by variations in NDBI values, and that in 2022, the coefficient variation values will likewise be the same. In general, there was a positive correlation between NDBI and LST values. Figure 4.22 below displays land surface temperature and NDBI a relationship for the years 2003 and 2022.

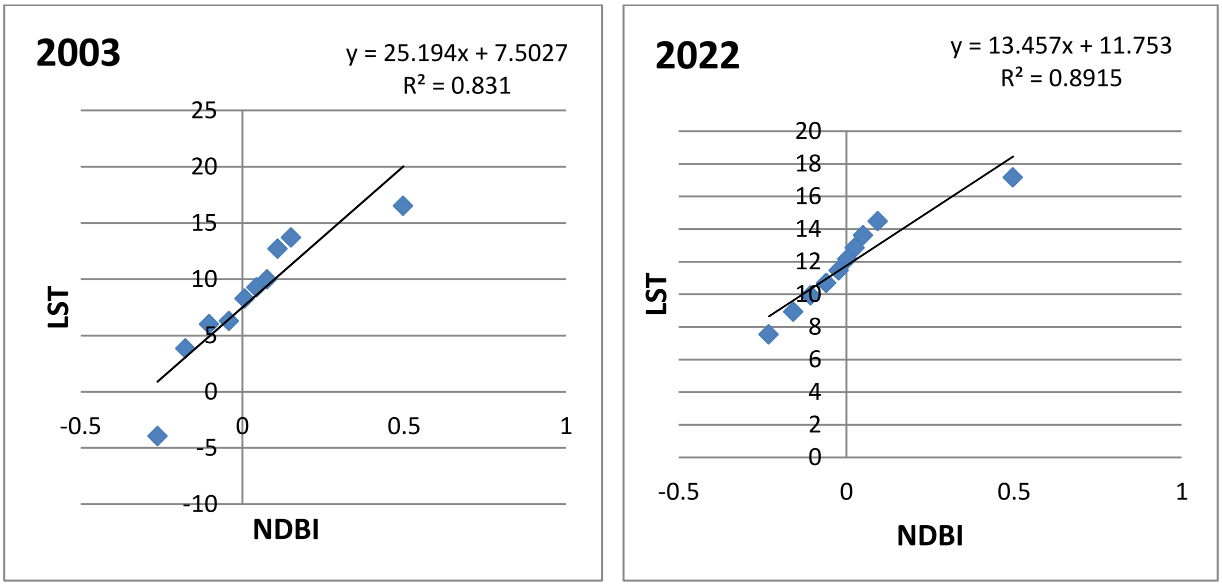

Fig 4.22 LST and NDBI correlation for Addis Ababa city

4.9.2 Relationship between normalized difference built- up index with land surface temperature of Adama city

There are direct correlation between NDBI and LST in the images from 2003, 2013, and 2022 that were examined. High LST is associated with high NDBI levels, and low LST with low NDBI. Over the period of the study, the R^2 values for the NDBI and LST correlations were 96.11%, 97.97%, and 87.14%, respectively. These results show that in 2003, variations in NDBI values accounted for 96.11% of LST variability and that in 2013 and 2022. In general, NDBI and LST values showed a positive correlation. The relationship between land surface temperature and NDBI for the years 2003, 2013, and 2022 is shown in Figure 4.23.

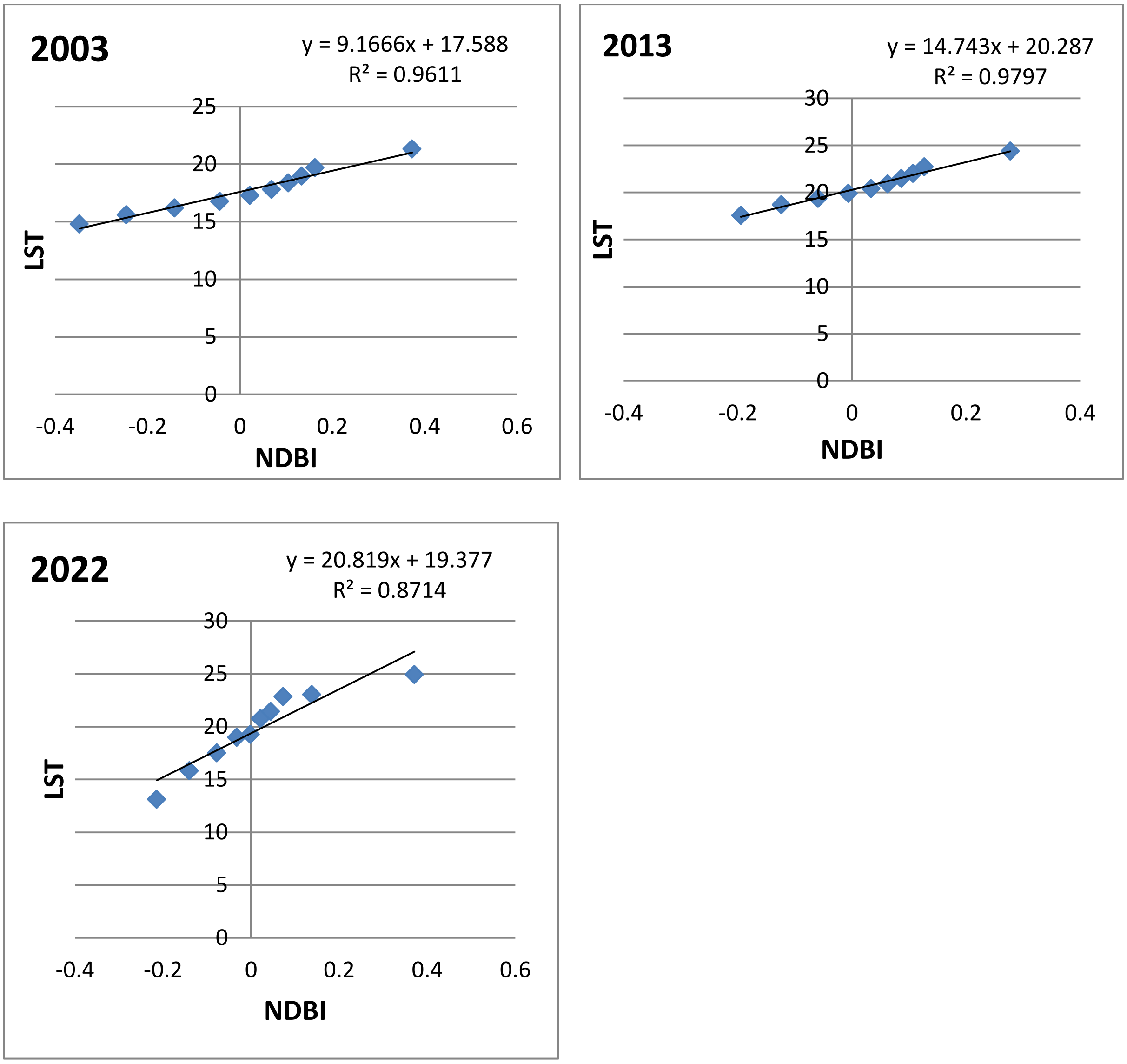

Fig 4.23 LST and NDBI correlation for Adama city

4.9.3 Relationship between normalized difference built- up index with land surface temperature of Hawassa city

In the images that were studied, there is a clear association between NDBI and LST for the years 2003, 2013, and 2022. Low LST is correlated with high NDBI levels, and vice versa. The R^2values for the NDBI and LST correlations during the course of the study were 96.83%, 98.81%, and 91.9%, respectively. These findings indicate that in 2003, as well as in 2013 and 2022, changes in NDBI values accounted for 96.83% of LST variability. In general, there was a positive correlation between NDBI and LST values. Figure 4.24 shows the correlation between LST and NDBI for the years 2003, 2013, and 2022.

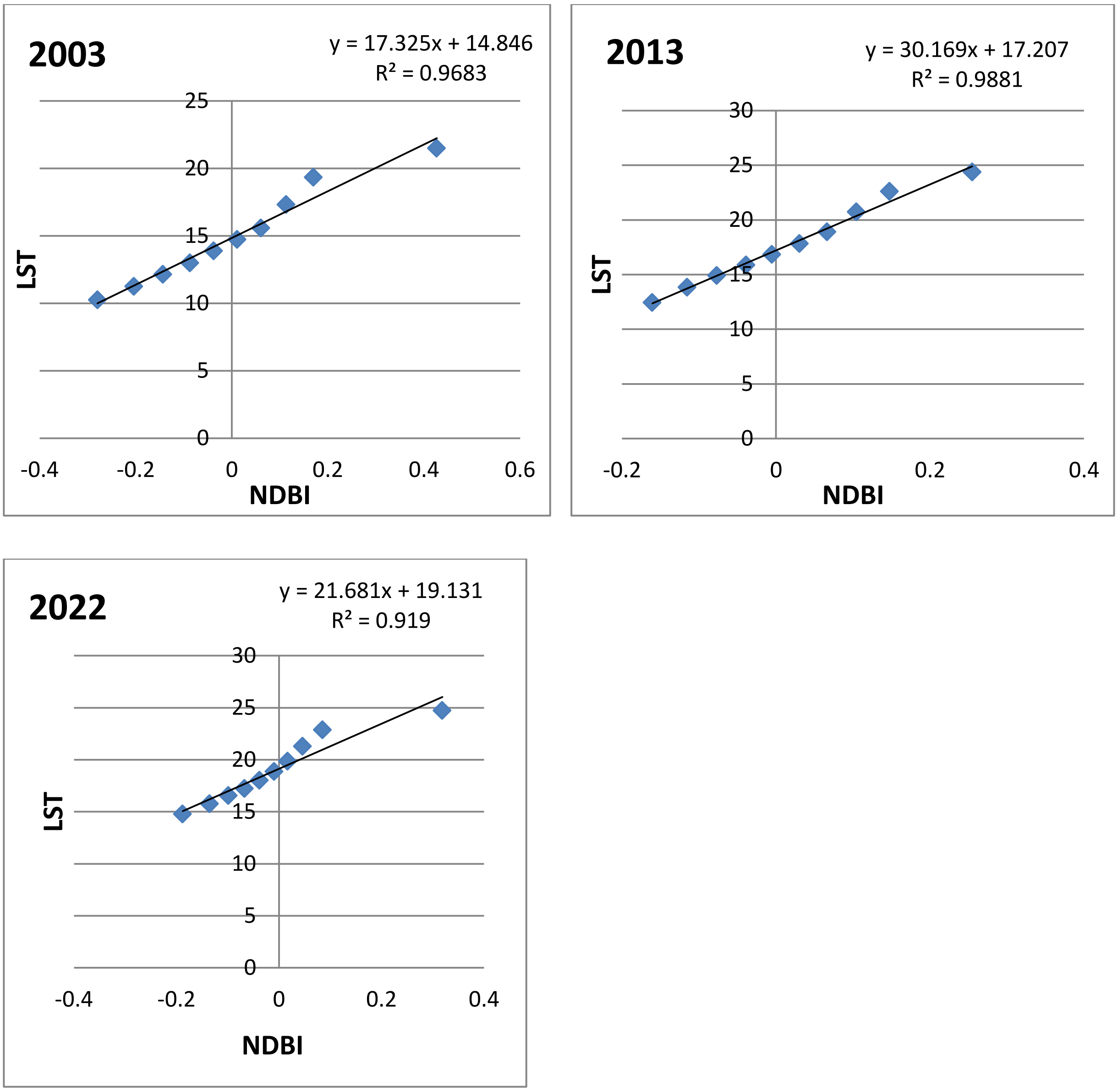

Fig 4.24 LST and NDBI correlation for Hawassa city

CHAPTER FIVE

5. Discussion

5.1 Land-use and land-cover status of study areas

The LULC variations seen in the three study regions (Addis Ababa, Adama, and Hawassa) indicate a relatively increasing need for land for settlement. Urban sprawl has come under criticism for its significant encroachment on agricultural land and inefficient use of energy and land resources. Urban sprawl is characterised as an area where urban development adversely affects the urban environment, which is neither appropriate for an agricultural rural environment nor an acceptable urban environment (Cheng, 2003). The environment has been negatively impacted by these changes in a number of ways. According to the research done by (Houghton R. , 1994), the main causes of LULC fluctuation are human population growth, economic development, technological advancement, and environmental changes. Changes in LULC are becoming substantial issues and a key contributor of environmental changes (FAO, 1999). (Alemayehu , 2008) It also showed some of the climate change data, such as the prevalence of drought, rising temperatures, floods, decreased yearly precipitation, and rising sea levels. The results of the present study shows that LULC experienced significant drastic change during the course of the 19-year study period. The area of the Addis Ababa region that is built-up has increased from 11693.43 ha in 2003 to 34766.1 ha in 2022. Additionally, the built-up areas in Adama and Hawassa increased from 1660.7 ha to 4281.18 ha and from 1164.17 ha to 5471.03 ha, respectively, between the years 2003 and 2022. In the reverse this study's findings indicate that agricultural land is really declining from 2003 to 2022. Between the years 2003 and 2022, the amount of agricultural land in Addis Ababa declined from 22800.26 ha to 10037.04 ha. Additionally, it demonstrates a reduction in Adama and Hawassa, from 7090.24 ha to 2389.07 ha and 4836.51 ha to 4094.7 ha, respectively. The growth in the area covered by built-up land can be explained by the clearing of agricultural land for the planting season and the clearing of agricultural land to make way for urban developments, especially housing and infrastructure.

5.2 Normalized difference vegetation index

Normalized difference vegetation index is a measure of vegetation condition and it is used also to determine LST. It is determined that NDVI is a reliable indication of LST and dryness (Mihai, 2012). The results of the present study also shows that the NDVI changed over time. In the three study areas, evidence suggests that the vegetation was healthier in 2003 than it was in the most recent year, 2022. This study examined the NDVI and LST correlation coefficient to provide insight into how the state of the vegetation affects the area's LST. LST will rise as the amount of vegetation decreases. In line with this, the present study revealed that NDVI have strong inverse relation with LST.

5.2.1 Relationship between normalized difference vegetation index with land surface temperature

In Addis Abba according to the examined images from 2003 and 2022, there are indirect (inverse) correlations between NDVI and LST. High LST is associated with low NDVI levels, and vice versa. The NDVI and LST correlations' R^2 values throughout the study period were 97.57% and 86.55%, respectively. These findings demonstrate that in 2003, 97.57% of LST variability was caused by variations in NDVI values, and that in 2022, the coefficient variation values will likewise be the same. In general, there was a negative correlation between NDVI and LST values. Figure 5.1 displays land surface temperature and NDVI a relationship for the years 2003 and 2022.

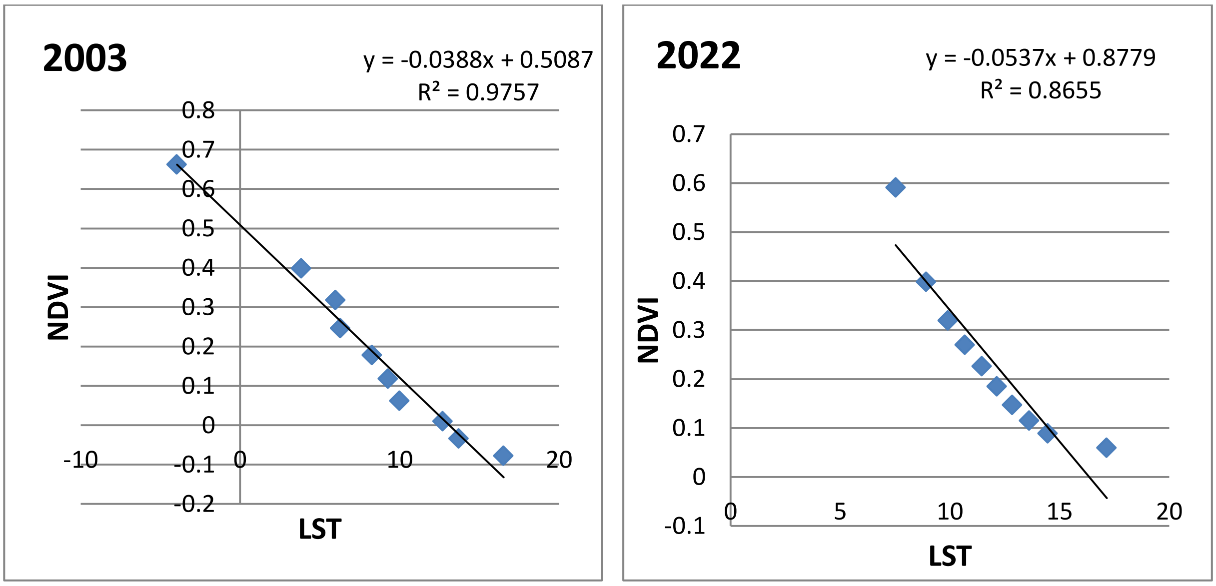

Fig 5.1 LST and NDVI correlation for Addis Ababa city

In Adama city there are indirect (inverse) relationships between NDVI and LST, according to the examined images from 2003, 2013, and 2022. Low NDVI values are related to high LST, and vice versa. Over the period of the study, the R^2 values for the NDVI and LST correlations were 86.68%, 89.38%, and 97.01%, respectively. These results show that in 2003, variations in NDVI values accounted for 86.68% of LST variability and that in 2013 and 2022. NDVI and LST values generally had negative correlations with one another. The relationship between land surface temperature and NDVI for the years 2003, 2013, and 2022 is shown in Figure 5.2.

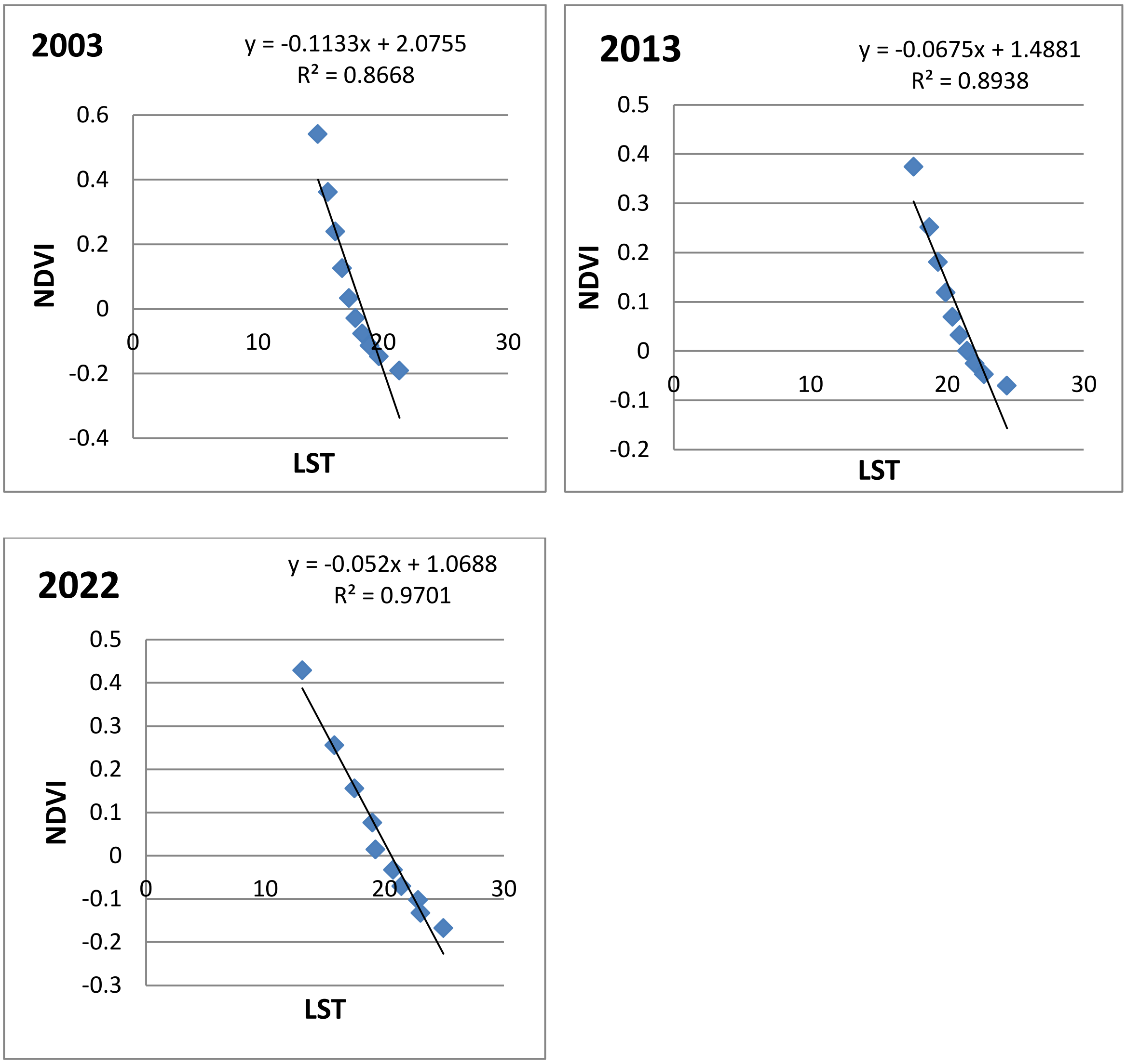

Fig 5.2 LST and NDVI correlation for Adama city

The studied images from 2003, 2013, and 2022 show indirect (inverse) correlations between NDVI and LST in Hawassa. High LST is correlated with low NDVI levels, and vice versa. The NDVI and LST correlations' R^2 values during the course of the study were 95.29%, 96.81%, and 93.46%, respectively. These findings indicate that in 2003, as well as in 2013 and 2022, fluctuations in NDVI values accounted for 95.29% of LST variability. In general, there was a negative correlation between NDVI and LST readings.

Figure 5.3 shows the correlation between land surface temperature and NDVI for the years 2003, 2013, and 2022.

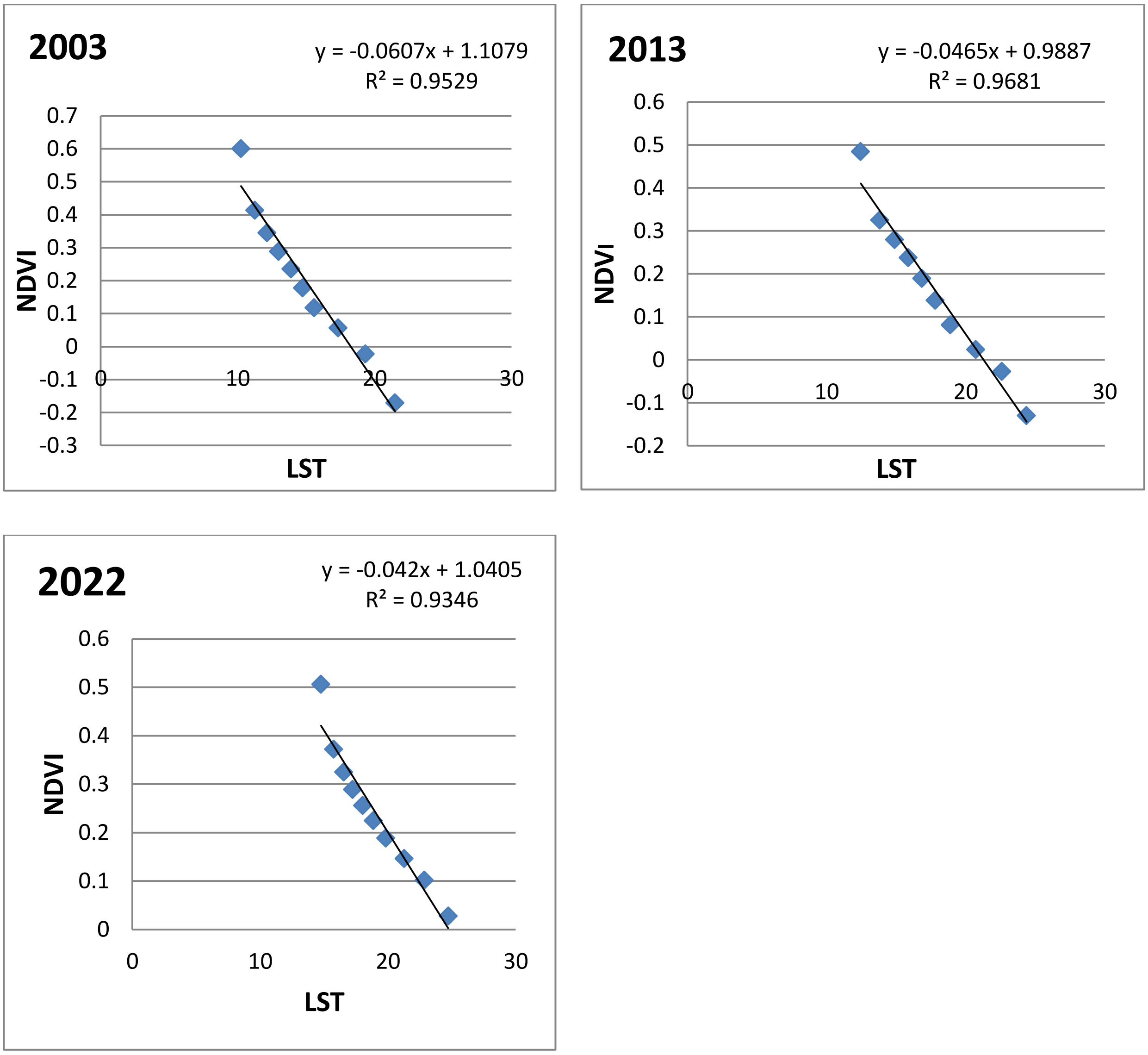

Fig 5.3 LST and NDVI correlation for Hawassa city

5.3 Normalized difference built-up index

Normalized difference built-up index (NDBI) is a remote sensing index that is commonly used as an indicator of urbanization. It measures the amount of built-up area within a given region by comparing the reflectance values of near-infrared and shortwave infrared bands. NDBI values range from -1 to 1, with higher values indicating more built-up areas. NDBI can be used to estimate the extent of urban areas, identify land-use changes, and monitor urban growth over time. It can also be used to assess the impact of urbanization on the environment, such as changes in surface temperature, vegetation cover, and water resources. The findings of this study indicate that the NDBI value has changed across the study periods from 2003 to 2022 in the specified areas of study. Because of that increase in NDBI during the course of the study's period, there has also been an increase in LST values in the study areas, as can be seen from the relationship between NDBI with LST.

5.4 Land surface temperature

This study examined LST of the study areas using a thermal band of an ASTER nighttime image. During night time, surface temperatures did not vary significantly, depending on the land cover type, compared with daytime (Bonggeun , 2015). Since it measures the temperature of the surface itself rather than the land use, the land surface temperature value of the ASTER night image doesn't change for various land use classes. The thermal characteristics of the surface material, the level of moisture present, and the time of day all have an impact on temperature. The results of the present study also shows that there is not a significant variation in the LST value across all LULC classes in each study periodes. The main reason for water bodies have high LST value is that Water does not cool easily at night time because the air temperature is usually cooler than the water temperature. This means that the water loses heat more slowly to the surrounding air, and therefore takes longer to cool down (Neha & Aneesh , 2018). The majority of images were collected during the dry season and during harvesting time, which is the main cause of the lower NDVI and higher LST values in the region of agricultural LU/LC class. The primary harvesting months in Ethiopia are November, December, and January. As a result, built-up areas, bare lands, and agricultural land have high surface reflectivity. The soil was extremely dry after grain harvest, and at the same time, land reflectance was also very high.

To evaluate the thermal status of land surface by satellite, it is important to find the relation between LULC type and LST. The primary causes of an increase in LST in both rural and urban regions are land-cover changes and haphazard use of land resources (Maitima, 2009) (Khin, 2012). With regard to LULC changes in the study area, with the expansion of settlements, agricultural lands have highly declined. This is clearly observed, especially in urban areas like Addis Ababa, Adama and Hawassa. The LST increased across the board for all significant LULC categories during the research period. Built-up and bare land areas had the largest mean LST change for the three study areas. The agricultural land had the lowest mean change LST, on the other hand.

CHAPTER SIX

6. Conclusion and Recommendations

6.1 Conclusion

This study was conducted to evaluate the impact of urbanisation on the environment (vegetation and land surface temperature) in three significant Ethiopian metropolitan districts (Addis Ababa, Adama and Hawassa). The study was done with the aim of analysing the impact using remote sensing and GIS techniques. Through examination of LULC, NDVI, NDBI, and LST variations over these times, Landsat and ASTER night time imageries from 2003, 2013, and 2022 were used to track the effects of urbanisation in the study areas. Data on land surface temperature and LULC produced from such data is crucial for tracking human activity and environmental changes. It was discovered that Landsat images are particularly helpful for measuring and mapping LULC change, NDVI, and NDBI in the study's areas, and that LST may also use ASTER night time images. The exploitation of environmental and socioeconomic elements through time and place has been ascribed to the LU/LC pattern in the study's areas. Because the study employs night time images, there is not a significant difference in the LST value across all LULC classes in each study period. Land-use/land-cover has been changing from time to time in the present study area. Land-use land-cover change has an impact on LST and NDVI. The LST minimum and maximum are increasing while the NDVI minimum and maximum are decreasing year after year. In order to detect temperature fluctuations, track LULC changes, and monitor environmental conditions, estimated LST is crucial. The results of this study demonstrated that, from 2003 to 2022, the NDVI of the studied regions decreased while the LSTs of the study areas increased. This was because of LULC changes, human activities and climate variability of the areas. The areas' land surface temperatures shows significant differences in LST between various LULC types. The LST indicate and vegetation coverage of the study's areas are also rather well-indicated by the NDVI values from satellite data. As a result, the study of the variations in LST, NDVI, and different LULC class patterns using GIS and remote sensing data in the study areas shows that it suggests a quicker and more economical approach with the benefit of covering a large area.

6.2 Recommendations

Based on Landsat and ASTER night time data from 2003, 2013, and 2022, the goal of this study was to evaluate and examine the impact of LULC changes on LST and vegetation in three major Ethiopian cities (Addis Abeba, Adama, and Hawassa). The study shown that LULC types may be converted to other LULC types, such as from agricultural areas to built-up areas. There are some circumstances, however, if the change could make a positive impact on LST and vegetation. Therefore, based on the result of this study, the following recommendations have been drawn.

- Taking high-resolution images for future studies in the study areas in order to accurately determine the LST, LULC relationship and detect LULC change.
- Land-use and land-cover change becomes a key part of current resource management and environmental change monitoring systems. Therefore, both governmental and non-governmental organizations should place a high priority on each LULC's ecological impact and proper land-use management.
- Making sustainable use of available land resources and preventing the loss of agricultural land due to uncontrolled horizontal expansion.
- Conservation measures must be done to protect the study area's urban green spaces, and it is advised that trees be planted and green spaces be marked off, especially in high-density population areas and bare land areas.
- The results of this study can be used as a foundation for future researchers who wish to investigate the effects of LULC changes and an increase in LST and decrease in vegetation on environmental problems and community livelihoods in the studied areas.

References

Canning, D. (2015). The State of Demographics in Sub-Saharan Africa. *World Bank Group*.

Cheng, J. (2003). Modelling Spatial and Temporal Urban Growth .

Di Gregorio, A., & Jansen , L. (2000). *Land cover classification system: classification concepts and user manuel.* FAO.

Houghton, R. (1994). The worldwide extent of land-use change. *BioScience*.

Lillesand, T. (2008). *Remote sensing and image interpretation.*

Alemayehu , M. (2008). Climate Variability and change. *Ethiopian journal of Animal*.

Angel, S. (2011). The dimensions of global urban expansion: Estimates and projections for all countries, 2000–2050. *Progress in Planning*.

Bonggeun , s. (2015). Analysis of Surface Temperature Accuracy in ASTER Images according to Land-Use Type. *Bureau of Ecological Conservation Research, National Institute of Ecology*.

Burgan, R., & Hartford, R. (1993). *Monitoring vegetation greenness with satellite data.* Department of Agriculture, Forest Service, Intermountain Research Station.

Chen, X. (2000). Using RS and GIS to analyze land-cover change and its impacts on the Regional Sustainable Development. *International Journal Remote Sensing*.

Chipman, J., & Lillesand, T. (2004). Mapping lake water clarity with Landsat images in Wisconsin, USA. *Canadian journal of remote sensing*.

Chithra. (2015). Impacts of Impervious Surfaces on the Environment. *International Journal of Engineering Science Invention*.

Congalton. (1991). A review of assessing the accuracy of classifications of remotely sensed data. *Remote sensing of enviroment*.

Cristóbal, J. (2009). Improvements in land surface temperature retrieval from the Landsat series thermal band using water vapor and air temperature. . *Journal of Geophysical Research*.

Du, C. (2015). A Practical Split-Window Algorithm for Estimating Land Surface Temperature from Landsat 8 Data. *Remote sensing*.

FAO, U. (1999). Terminology for integrated resources planning and management. *Food and agriculture organization/United Nations Environmental program*.

Foody, G. (2022). Status of land cover classification accuracy assessment. *Remote sensing of environment*.

Foresman, T. (1998). The history of geographic information systems : perspectives from the pioneers. *Semantic scholar*.

Forman, R. (2016). Urban ecology principles: are urban ecology and natural area ecology really different. *Landscape ecology*.

Fu, P., & Weng, Q. (2016). A time series analysis of urbanization induced land use and land cover change and its impact on land surface temperature with Landsat imagery. . *Remote Sensing of Environment*.

Hardegree, L. (2006). *Spatial Characteristics Of The Remotely-sensed Surface Urban Heat.* Doctoral dissertation.

Houghton, R. (1994). The worldwide extent of land-use change. *BioScience*.

Huisman, O., & De By, R. (2009). *Principles of geographic information systems.*

Ibrahim, F., & Rasul, G. (2017). Urban Land Use Land Cover Changes and Their Effect on Land Surface Temperature: Case Study Using Dohuk City in the Kurdistan Region of Iraq. *Climate*.

Jiménez-Muñoz. (2008). Split-window coefficients for land surface temperature retrieval from lowresolution thermal infrared sensors. . *IEEE Geoscience Remote Sensing Letters.*

Kayet, N., Pathak, K., & Chakrabarty, A. (2016). Spatial impact of land use/land cover change on surface temperature distribution in Saranda Forest, Jharkhand. *Modeling Earth Systems and Environment*.

Kern, A. (2011). *Deriving Normalized Difference Vegetation Index based on remotely sensed.* Doctoral dissertation, Eötvös Loránd University.

Kerr, Y., Lagouarde, J., & Nerry, F. (2004). Land surface retrieval techniques and applications: case of AVHRR, in: Quatrocci, D.A., Luvall, J. C. *Thermal remote sensing in land surface processes. CRC press, Florida,.*

Khin, M. (2012). Land surface temperature changes by LU changes of Inlay Lake area, Myanmar. *Department of Spatial Information Engineering, Pukyong National University, South Korea.*

Khin, M.Y, M., Shin , D., & Park, J.J, J. (2012). Land surface temperature changes by LU changes of Inlay Lake area, Myanmar. *Department of Spatial Information Engineering, Pukyong National University, South Korea.*

Komba, W., & Keribich, V. (2000). Reconciling informal and formal land management:: an agenda for improving tenure security and urban governance in poor countries. *Habitat International*.

Kumar, R., & Singh, S. (2016). Case Study for Change Detection Analysis and Land Surface Temperature Retrieval in Uttrakhand Region and their correlation. *Imperial Journal of Interdisciplinary Research*.

Lambin, , E., & Meyfroidt, P. (2010). Land use transitions: Socio-ecological feedback versus socio-economic change. *Elsevier Sci Ltd (Oxford).*

Lambin, E., & Turner, B. (2001). The causes of land-use and land-cover change: moving beyond the myths. *Global environmental change*.

Lamson-Hall, P. (2022). The Ethiopia Urban Expansion Initiative and knowledge exchange. *Buildings & cities*.

Latif, M. (2014). Land Surface Temperature Retrival of Landsat-8 Data Using Split Window Algorithm-A Case Study of Ranchi District. *International Journal of Engineering Development and Research*.

Li, J., Song, C., & Zhu, F. (2011). Impacts of landscape structure on surface urban heat islands: A case study of Shanghai, China. *Remote Sensing of Environment*.

Li, J., Liu, Y., & Cao, M. (2015). Space-time characteristics of vegetation cover and distribution: case of the Henan province in China. *Sustainability*.

Li, Z. (2013). Satellite-derived land surface temperature:Current status and perspectives. *Remote Sensing of Environment*.

Lillesand, T., & Kiefer, R. (2017). Remote Sensing and Image Interpretation. *Journal of Geographic Information System*.

Madanian, M. (2018). The study of thermal pattern changes using Landsat-derived land surface temperature in the central part of Isfahan province. *Sustainable Cities and Society*.

Maitima, J. (2009). The linkage between land-use change, land degradation and biodiversity across East Africa. *Africa Journal of environmental science and technology*.

Mather, A., & Needle, C. (2000). The relationships of population and forest trend. *The Geographical Journal*.

Meyer, W., & Turner, B. (1992). . Human population growth and global land-use/cover. *Annual review of ecology and systematics*.

Mihai, V. (2012). Using Satellite Images Landsat TM For calculating Normalized Difference Indexes for the landscape of Parang mountains. *Banat University of Agricultural sciences and Veterinary medicine, Romania*.

Muhammad Yazrin Yasin. (2020). Land Cover and NDBI analysis to map built up area in Iskandar Malaysia. *Earth and Environmental Science*.

Neha , G., & Aneesh , M. (2018). Analysis of cooling effect of water bodies on land surface temperature in nearby region: A case study of Ahmedabad and Chandigarh cities inIndia. *The Egyptian Journal of Remote Sensing and Space Sciences*.

Paramasivam, C. (2016). Remote Sensing and spectral studies of magnesite mining area, Salem, India. *For the award of the Degree of Doctor of Philosophy in Geology thesis submitted to Periyar University, Salem, India*.

Pickett, S. (2001). Urban Ecological Systems: Linking Terrestrial Ecological, Physical, and Socioeconomic Components of Metropolitan Areas. *Annual Review of Ecology and Systematics*.

Rajeshwari, A., & Mani, N. (2014). Estimation of land surface temperature of Dindigul Woreda using Landsat 8 data. *International Journal of Research in Engineering and Technology*.

Reddy, S., & Manikiam, B. (2017). Land Surface Temperature Retrieval from LANDSAT data using Emissivity Estimation. *International Journal of Applied Engineering Research*.

Rose, N. (2022). An introduction to zonal statistics.

Sameh , W., & Guang , Z. (2015). *Ethiopia urbanization review.* World band group.

Santa , P. (2011). Forest Cover and Land Use Changes: A Study of Laljhadi Forest (Corridor), Far-Western Development Region, Nepal. *MSc Thesis Tribhuvan University*.

Tayyebi, a. (2018). Analyzing long-term spatio-temporal patterns of land surface temperature in response to rapidurbanization in the mega-city of Tehran. *Land Use Policy*.

UN. (2022). *World Population Prospects 2022: Summary of Results.* United Nations Department of Economic and Social Affairs, Population Division (2022).

UNCED. (1992). United Nations Conference on Environment & Development.

USAPA. (2004). A Summary of Models for assessing the effects of Community Growth and change on land-use patterns. *Environmental protection Agency office of research and development*.

VALDIVIEZO-N, J. C. (2017). Built-up index methods and their applications. *Journal of the Optical Society of America A.*

Voogt, J. (2000). How researchers measure UHI. *Glossary of Meteorology, 2nd edition, Canada.*

Wang, S. (2018). Detection of urban expansion and land surface temperature change using multi-temporal landsat images. *Resources,Conservation and Recycling*.

Weng, Q. (2019). Normalizing Land Surface Temperature for environmental parameters in mountainous and urban areas of a cold semi-arid climate. *Science of the Total Environment*.

Yu, Z., Guo, X., & Zeng, Y. (2015). Variations in land surface temperature and cooling efficiency of green space in rapid urbanization: The case of Fuzhou city, China. *Urban Forestry & Urban Greening*.

Zhao, W. (2019). Normalization of the temporal effect on the MODIS land surface temperature product using random forest regression. *ISPRS Journal of Photogrammetry and Remote Sensing*.

ZHOU, X., & WANG, Y.-C. (2010). Dynamics of Land Surface Temperature in Response to Land-Use/Cover Change. *Geographic research*.

Zubair, A. (2006). Change detection in LU/LC using RS data and GIS a case study of Ilorin. *Department of geography, University of Ibadan.*

Appendices

Appendix 1: Values used for relationship of NDBI with LST, NDBI with NDVI and NDVI with LST for Addis Ababa 2003

NDBI	LST	NDVI
-0.26198757	-3.9618219	0.662337661
-0.17627209	3.84666802	0.398302507
-0.10280167	5.9907424	0.318291855
-0.04157633	6.27734195	0.246282268
0.00740395	8.27811656	0.178273213
0.044139158	9.27889117	0.118265224
0.076792676	9.99384083	0.062257767
0.109446194	12.7087905	0.010250843
0.150263091	13.70956511	-0.033755016
0.497206718	16.52853882	-0.077760875

Appendix 2: Values used for relationship of NDBI with LST, NDBI with NDVI and NDVI with LST for Addis Ababa 2022

NDBI	LST	NDVI
-0.231198139	7.536963968	0.5911749
-0.157982084	8.922391645	0.398372374
-0.106730845	9.9229783	0.319498613
-0.059140409	10.69266034	0.269837356
-0.022532382	11.46234239	0.2260186
0.003093237	12.15505622	0.185121094
0.025058054	12.84777006	0.147144839
0.050683673	13.61745211	0.115011085
0.094613306	14.46410235	0.088719831
0.497301608	17.1579895	0.059507327

Appendix 3: Values used for relationship of NDBI with LST, NDBI with NDVI and NDVI with LST for Adama 2003

NDBI	LST	NDVI
-0.347350049	14.78826904	0.541401267
-0.246025068	15.5958252	0.361114574
-0.141081337	16.19229126	0.239697005
-0.043375105	16.74633789	0.125638076
0.021762383	17.2835083	0.033655069
0.068806124	17.79818726	-0.028893376
0.104993617	18.34555054	-0.076724539
0.133943612	18.94204712	-0.113517742

0.162893607	19.68408203	-0.146631624
0.372781068	21.30218506	-0.190783468

Appendix 4: Values used for relationship of NDBI with LST, NDBI with NDVI and NDVI with LST for Adama 2013

NDBI	LST	NDVI
-0.194395418	17.55541669	0.37414965
-0.123458598	18.70887343	0.251709011
-0.059172104	19.35480921	0.180822325
-0.005969489	19.90846845	0.118527965
0.033932472	20.41598942	0.069122093
0.062750555	20.92351038	0.032604709
0.087135087	21.47716962	0.000383488
0.107086068	22.03082886	-0.025393488
0.127037048	22.7229029	-0.046874302
0.277777791	24.38388062	-0.070503198

Appendix 5: Values used for relationship of NDBI with LST, NDBI with NDVI and NDVI with LST for Adama 2022

NDBI	LST	NDVI
-0.214054897	13.11435333	0.428571433
-0.140201602	15.80223537	0.255221654
-0.077710352	17.49710579	0.155325171
-0.03226217	18.98011741	0.075995612
-0.001016546	19.25127023	0.014294843
0.021707545	20.73428185	-0.032715266
0.044431636	21.42915227	-0.07091098
0.07283675	22.81889311	-0.103230431
0.138168511	23.02209241	-0.132611749
0.371090442	24.93001916	-0.167869331

Appendix 6: Values used for relationship of NDBI with LST, NDBI with NDVI and NDVI with LST for Hawassa 2003

NDBI	LST	NDVI
-0.279458928	10.2435292	0.600000024
-0.203937473	11.24726275	0.413911269
-0.143520309	12.14534015	0.345552134
-0.086879218	12.99058946	0.288586189
-0.037790272	13.88866685	0.235417973
0.011298674	14.73391616	0.178452028
0.06038762	15.57916547	0.117688353
0.113252638	17.32249217	0.056924678
0.16989373	19.32995929	-0.022827646
0.426666677	21.49591064	-0.170939104

Appendix 7: Values used for relationship of NDBI with LST, NDBI with NDVI and NDVI with LST for Hawassa 2013

NDBI	LST	NDVI
-0.160479107	12.44878229	0.484662563
-0.115121403	13.81883629	0.325105248
-0.076925441	14.90346237	0.279947517
-0.038729479	15.87391728	0.237800302
-0.005308013	16.8443722	0.189632056
0.030500701	17.81482711	0.138453295
0.066309415	18.8994532	0.081253503
0.104505377	20.72619186	0.024053711
0.147475833	22.61001611	-0.027125051
0.254901975	24.37966919	-0.129482573

Appendix 8: Values used for relationship of NDBI with LST, NDBI with NDVI and NDVI with LST for Hawassa 2022

NDBI	LST	NDVI
-0.187563838	14.76499993	0.505689323
-0.135091726	15.75063153	0.371683485
-0.098361247	16.53913682	0.324781442
-0.06687798	17.22907894	0.289046552
-0.038018318	18.01758423	0.255545093
-0.009158656	18.85537109	0.224277064
0.0170774	19.8410027	0.188542174
0.045937062	21.27016853	0.146106992
0.085291146	22.8471791	0.10143838
0.318792045	24.71987915	0.027735169

Appendix 9: Classification accuracy assessment report of Addis Ababa for the year 2003

LULC	Built-up	Bare land	Agricultural	Forest	Water body	TOTAL(User)
Built-up	30	2	2	0	0	34
Bare land	3	19	0	0	0	22
Agricultural	0	8	35	0	0	43
Forest	0	0	0	10	9	19
Water body	0	0	0	2	10	12
TOTAL(Producer)	33	30	37	12	19	130

Appendix10: Classification accuracy assessment report of Addis Ababa for the year 2013

LULC	Built-up	Bare land	Agricultural	Forest	Water body	TOTAL(user)
Built-up	31	0	5	0	0	36
Bare land	2	18	3	0	0	23
Agricultural	12	0	25	0	0	37

Forest	0	0	0	16	6	22
Water body	0	0	0	3	9	12
TOTAL(Producer)	45	18	30	19	15	130

Appendix11: Classification accuracy assessment report of Addis Ababa for the year 2022

LULC	Built-up	Bare land	Agricultural	Forest	Water body	TOTAL(user)
Built-up	44	2	3	0	0	49
Bare land	0	14	3	0	0	17
Agricultural	2	3	23	0	0	28
Forest	0	0	0	17	4	21
Water body	0	0	0	2	13	15
TOTAL(Producer)	46	19	29	19	17	130

Appendix12: Classification accuracy assessment report of Adama for the year 2003

LULC	Forest	Water body	Agriculture	Bare land	Built-up	TOTAL(user)
Forest	8	0	0	3	0	11
Water body	3	9	0	3	0	15
Agriculture	0	0	33	6	0	39
Bare land	0	0	0	15	0	15
Built-up	0	0	3	3	14	20
TOTAL(P)	11	9	36	30	14	100

Appendix13: Classification accuracy assessment report of Adama for the year 2013

LULC	Built-up	Bare land	Agricultural	Forest	Water body	TOTAL(user)
Built-up	21	3	2	0	0	26
Bare land	2	15	2	0	0	19
Agricultural	0	2	20	0	5	27
Forest	0	2	1	12	0	15
Water body	0	0	3	0	10	13
TOTAL(Producer)	23	25	33	12	15	100

Appendix14: Classification accuracy assessment report of Adama for the year 2022

LULC	Agriculture	Water body	Bare land	Built-up	Forest	TOTAL(user)
Agriculture	10	6	4	0	0	20
Water body	4	12	0	0	0	16
Bare land	0	0	18	0	0	18
Built-up	0	0	2	28	0	30
Forest	0	0	3	0	13	16
TOTAL(Producer)	14	18	27	28	13	100

Appendix15: Classification accuracy assessment report of Hawassa for the year 2003

LULC	Built-up	Bare land	Agricultural	Forest	Water body	TOTAL(user)
Built-up	10	10	0	0	0	20
Bare land	0	15	0	0	0	15
Agricultural	0	0	12	0	0	12
Forest	0	7	3	25	0	35
Water body	0	0	0	3	15	18
TOTAL(Producer)	10	32	15	28	15	100

Appendix16: Classification accuracy assessment report of Hawassa for the year 2013

LULC	Built-up	Bare land	Agricultural	Forest	Water body	TOTAL(user)
Built-up	12	3	2	0	0	17
Bare land	0	13	6	0	0	19
Agricultural	0	5	26	0	0	31
Forest	0	2	1	14	0	17
Water body	0	4	0	2	10	16
TOTAL(Producer)	12	27	35	16	10	100

Appendix17: Classification accuracy assessment report of Hawassa for the year 2022

LULC	Built-up	Bare land	Agricultural	Forest	Water body	TOTAL(user)
Built-up	21	2	1	0	0	24
Bare land	2	17	3	0	0	22
Agricultural	0	6	19	0	0	25
Forest	0	3	2	13	0	15
Water body	0	0	0	2	12	14
TOTAL(Producer)	23	28	25	15	12	100